The Abdus Salam
International Centre for Theoretical Physics

United Nations
Educational, Scientific and
Cultural Organization

IAEA
International Atomic Energy Agency

2327-10

Joint ICTP-IAEA Workshop on Fusion Plasma Modelling using Atomic and Molecular Data

23 - 27 January 2012

Modelling of warm dense matter and the transition from condensed matter to warm dense matter regime

Beata ZIAJA-MOTYKA

HASYLAB at DESY, Notkestr. 85
D-22603 Hamburg
GERMANY

Modelling of warm dense matter and the transition from condensed matter to warm dense matter regime

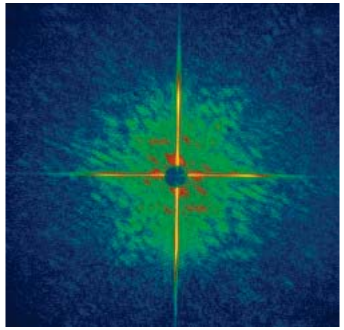

Beata Ziaja

Center for Free-Electron Laser Science, DESY

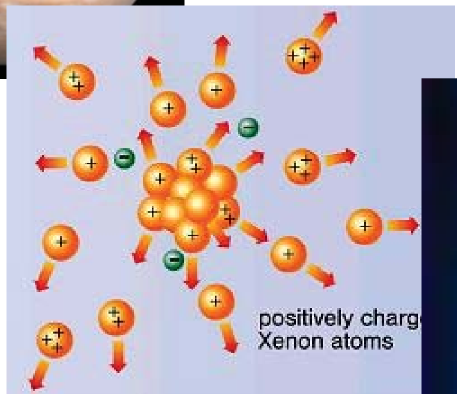

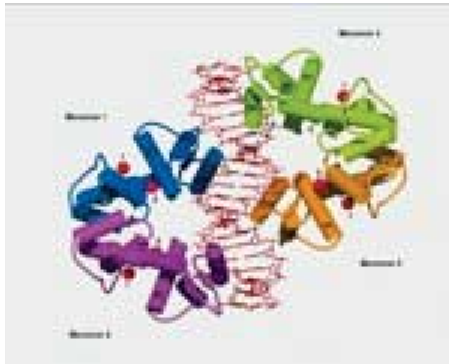

HELMHOLTZ ASSOCIATION

CFEL SCIENCE

DESY

Theory Group
at Center for Free-Electron Laser Science

The CFEL Theory Division develops theoretical and computational tools to predict the behavior of matter exposed to intense electromagnetic radiation. We employ quantum-mechanical and classical techniques to study ultrafast processes that take place on time scales ranging from picoseconds (10-12 s) to attoseconds (10-18 s). Our research interests include the dynamics of excited many-electron systems; the motion of atoms during chemical reactions; and x-ray radiation damage in matter.

Members of the CFEL Theory Division (from left to right): Zoltan Jurek, Oriol Vendrell, Sang-Kil Son, Stefan Pabst, Arina Sytcheva, Otfried Geffert, Robin Santra (Division Director), Mohamed El-Amine Madjet, Beata Ziaja-Motyka, Gopal Dixit, Marc Caballero; **Recently joined:** Nikita Medvedev, Robert Thiele, Jan Slowik, Zheng Li

HELMHOLTZ ASSOCIATION CFEL SCIENCE DESY

Radiation from FELs explores:

- Ultrasmall spatial scales: the structure of objects down to atomic resolutions

- Ultrashort temporal scales: transitions occurring at timescales down to femtoseconds

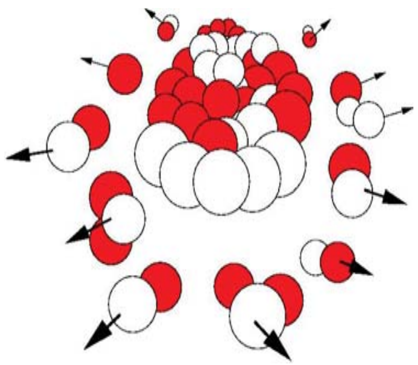

Unravelling magnetization

Study various aspects of magnetization – with possible applications in data storage ...

Observing small objects in strong fields

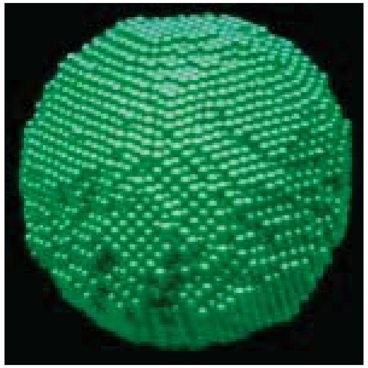

Novel experiments with atoms, molecules, ions or clusters. Particles excited into new, previously unknown states ...

Creating and investigating plasmas

Plasmas created that are as hot as the interiors of giant stars. Also probing evolution of plasmas ...

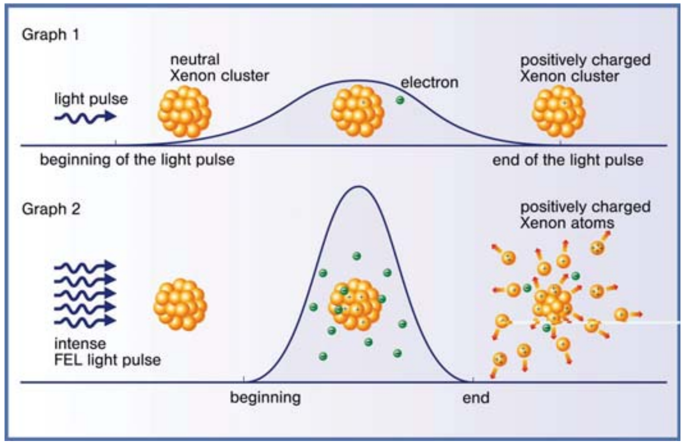

Deciphering the structure of biomolecules

3D structure of non-crystallizing biomolecules, cell constituents and whole viruses. This will provide the basis for future medicines ...

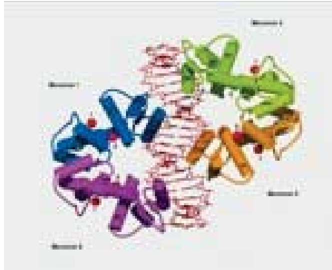

Exploring the nanoworld in 3D

Novel, three-dimensional insights into the nanoworld and thus shed light on future technological applications ...

Filming chemical reactions

Probing chemical reaction triggered by a laser flash ...

Content

- Physical mechanisms of radiation induced dynamics within samples irradiated with VUV, soft- and hard X-rays

- Models: particle approach → Monte Carlo (MC) code to describe spatio-temporal characteristics of Auger-electron cascades in solids

  Models: transport approach → semiclassical kinetic Boltzmann code to describe dynamics within atomic clusters irradiated at 100 nm, 32 nm and 13 nm wavelength.

  Models: combined TBMD-MC-Boltzmann model -> structural changes in irradiated solids

I. Mechanisms

Evolution of irradiated samples

Two phases:

- non-equilibrium ionization phase: starts with the photon irradiation and lasts until thermalization of electrons is reached

- semi-equilibrium expansion phase: electron plasma in local thermodynamic equilibrium, ions and electrons slowly thermalize.

- for finite samples: escape from outer shells → expansion of the sample

Induced dynamics

Contribution of different processes to dynamics strongly depends on radiation wavelength

Dynamics induced by VUV photons

Basic processes contributing:

- photoionizations (from outer shells) and collisional ionizations, elastic scatterings of electrons on atoms/ions
- long-range Coulomb interactions of charges with external and internal fields
- heating of electrons by inverse bremsstrahlung
- modification of atomic potentials by electron screening and ion environment
- recombination (3-body recombination)
- short range electron-electron interactions

Atomic data!

DESY

Dynamics induced by VUV photons

Also other processes may contribute:

- multiphoton ionization
- many-body recombination
- ionization by internal electric field at the edge of the sample
- ....

Dynamics induced by VUV photons

Specific interactions in detail:

plasma effects

Plasma created by VUV photons

No experimental evidence on electron temperatures from first FEL experiment

At early stages:
cold, dense plasma
→ strongly coupled, degenerate plasma
(quantum treatment of many body interactions necessary)

→
heats up

At later stages:
warm plasma→ classical, ideal plasma (can be treated classically)

⇓

Difficult unified treatment of these two regimes

Plasma created by VUV photons

If heating mechanism efficient, classical treatment justified

In any case we shall monitor Coulomb coupling and degeneracy parameters during the exposure ...

Plasma created by VUV photons

Cold, dense plasma effects

–degenerate: quantum statistics have to be used

–strongly coupled: electron and ions are quasiparticles with density dependent self-energies moving inside a dense interacting medium

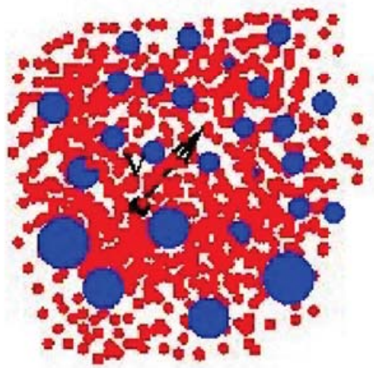

Screening by electron-ion medium:
depends on impact velocity, $\mathbf{v}$

$$V_{eff}(\mathbf{k},\omega) = \frac{V_{coul}(\mathbf{k})\,\delta(\omega - \mathbf{kv})}{\epsilon_e(\mathbf{k},\mathbf{kv}) + \epsilon_i(\mathbf{k},\mathbf{kv}) - 1}$$

Static, if $\mathbf{kv} \approx 0$

Dynamic, if $\omega_e >> \mathbf{kv} >> \omega_i$ ← only electrons,

if $\omega_e >> \omega_i >> \mathbf{kv}$ ← electrons and ions,

ω_e, ω_i are plasma frequencies for electrons and ions

Plasma created by VUV photons

Effects of strong coupling and degeneracy:

–self energy of quasiparticles: electronsand ions

–lowering of continuum level

–lowering of ionization thresholds

–merging of bound states into continuum at high densities (Mott effect)

–dynamic screening

–changes in photo-, collisional, and recombination rates

–Pauli blocking (phase-space occupation effects) at high densities

-multielectron recombination [Ziaja, Wang, Weckert]

Plasma created by VUV photons

Proper treatment of cold dense plasma possible with complicated quantum kinetic equation: [Bornath, Kraeft, Schlanges et al.]

Some dense plasma effects can be included into our semi-classical model:

–quasiparticle self energies

–lowering of continuum level

–lowering of ionization thresholds

–changes in photo-, collisional, and recombination cross sections due to the screening

Dynamics induced by VUV photons

Specific interactions in detail:

inverse bremsstrahlung

Inverse bremsstrahlung

Classical impact model to start with:

elastic scatterings of electron on ions → gain of electron thermal energy due to momentum transfer

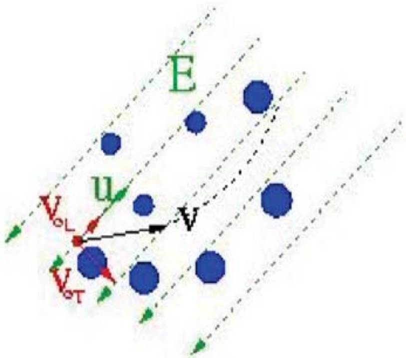

Initial and final electron velocities:

$\mathbf{v} = \mathbf{u} + \mathbf{v_0}$ and $\mathbf{v}' = \mathbf{u} + \mathbf{v}_0'$

$\mathbf{v_0}$, $\mathbf{v}_0'$, thermal velocities,

$\mathbf{u} = -\frac{e\,\mathbf{E_0}}{m\omega} sin(\omega t)$, quiver velocity,

where $E = E_0 \epsilon\, cos(\omega t)$, strength of electri field of polarization ϵ

↓

Thermal energy gain, $\Delta\mathcal{E}_0 = -m\mathbf{u}(\mathbf{v}_0' - \mathbf{v_0})$

Inverse bremsstrahlung

Quantum emission or absorption of n photons [Kroll, Watson]:

$$\left(\frac{d\sigma}{d\Omega}\right)_{n,i}(\mathbf{v}_0, \mathbf{v}_0'; n\hbar\omega) \sim J_n{}^2\left(-\frac{e E_0}{m\omega}\frac{\epsilon \mathbf{Q}}{\hbar\omega}\right) \cdot |\, U(\mathbf{Q})\,|^2,$$

where:

$\mathbf{Q} = m(\mathbf{v}_0' - \mathbf{v}_0)$, momentum transfer

$s = \frac{e E_0}{m\omega}\frac{1}{\hbar\omega}$, field strength parameter

$\mathcal{E}_0' = \mathcal{E}_0 + n\hbar\omega$ $(|\, n\,| > 0)$, energy gain or loss

$U(\mathbf{Q})$, Fourier transform of the interaction potential, $U(\mathbf{r})$: for point-like ions

or smooth ion charge density [Santra,Greene]

Inverse bremstrahlung

Field strength parameter, s:

$s << 1 \rightarrow J_n^2(sx) \sim (sx)^{2n} \rightarrow$ one-photon exchanges dominate

$s > 1 \rightarrow$ many-photon exchanges take place $\rightarrow$ limiting case can be identified with the classical impact picture

Dynamics induced by X-ray photons

Other processes than in VUV case give dominant contribution to radiation damage: inner and outer shell ionizations. No inverse bremsstrahlung.

Warm/hot plasma can be created.

Dynamics induced by X-ray photons

Basic processes contributing:

- photoionizations (from outer and inner shells with subsequent Auger decays) and collisional ionizations, elastic scatterings of electrons on atoms/ions
- long-range Coulomb interactions of charges with internal fields
- modification of atomic potentials by electron screening and ion environment
- recombination (3-body recombination)
- short range electron-electron interactions
- Compton scattering
- ionization by internal electric field at the sample edge

No inverse bremsstrahlung at these radiation wavelengths.

Radiation damage by X-ray photons

Specific interactions in detail:

photo- and collisional ionizations

Photoionizations

Photoelectric effect: the dominant source of radiation damage (~90 % of interactions for light elements C, N, O, S)

5% of photoemissions: outer-shell event, single electron emitted

95% of events: inner-shell event, Auger effect

Auger effect

$\Downarrow$

K-hole (lifetime 1-10 fs)

$\Downarrow$

L-shell electrons fall into K-hole

$\Downarrow$

energy transfer

$\Downarrow$

Auger electron $E \sim 0.25 keV$

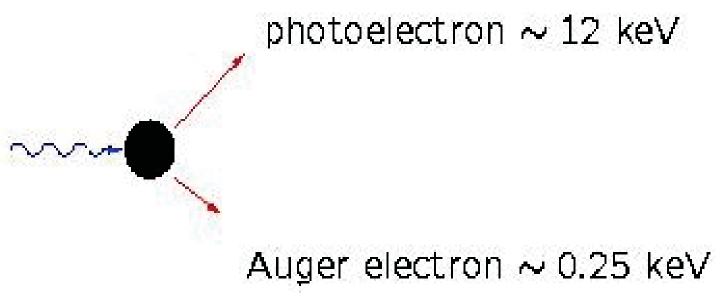

Collisional ionization by electrons

Two energy regimes of electrons released by X-ray photons:

- Photoelectrons: $E = 12$ keV, $\lambda_{DeBroglie} \approx 0.1$ Å, fast, propagate almost freely through the medium, leave small samples (10-100 nm) in a few femtoseconds

- Auger electrons: $E = 0.25$ keV, $\lambda_{DeBroglie} \approx 0.8$ Å, slow, interact multiply with neighbouring atoms, interaction includes exchange terms

Auger electrons are the main source of secondary ionization

Collisional ionizations by electrons

Primary ionization
(photo- and Auger)

Secondary ionization

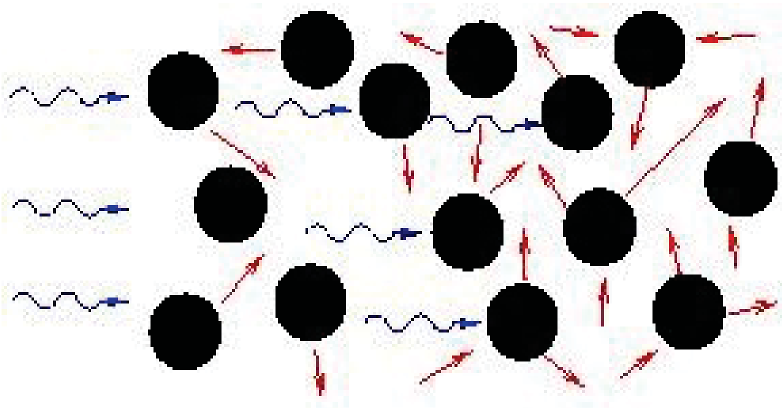

Photons

Electrons

II. Models

Particle approach

Solving equations of motion for each particle at each time step

$$\frac{d\mathbf{r}}{dt} = \mathbf{v}$$

$$\frac{d\mathbf{v}}{dt} = \mathbf{a}$$

Results are averaged over the total numer of simulated events

Scattering probabilites: obtained with cross sections

Particle approach

Advantages:

- first-principles model
- transparent algorithm
- no complex numerics

Disadvantages:

- high computational costs which scale with the number of participating particles
- statistical errors

Particle approach

Methods:

- stochastic Monte-Carlo method
- deterministic Molecular Dynamics simulations
- Particle-in-Cell method

Particle approach

Example: MC code for modelling Auger-electron cascade in diamond [Ziaja et al.]

Electrons interact multiply with atomic clusters:

- elastically - with no energy loss

$$\lambda_{elast} \sim \frac{1}{\sigma_{elast}}$$

- inelastically - with energy loss ω, either transferred to a cluster, or to another electron

$$\lambda_{inelast} \sim \frac{1}{\sigma_{inelast}}$$

$\Downarrow$

Cascade of secondary electrons

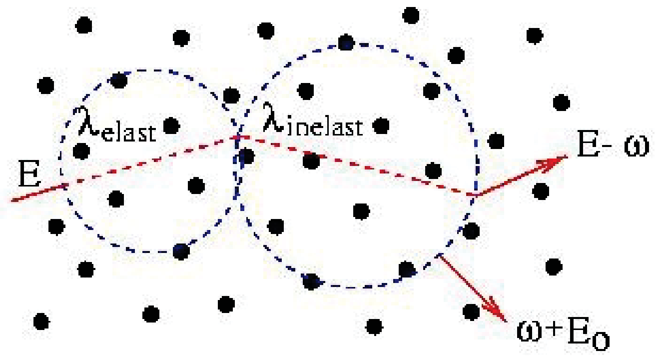

Particle approach

Example: MC code for modelling Auger-electron cascade in diamond

- Elastic collisions: muffin-tin potential, partial wave expansion, phase shifts δ_l

$$\sigma_{elast} = \frac{4\pi}{k^2} \sum_{l=0}^{\infty} (2l+1) \sin^2 \delta_l$$

$$\Downarrow$$

$$\lambda_{elast} \sim \frac{1}{\sigma_{elast}}$$

- Inelastic collisions: optical models based on an atomic-oscillator model of dispersive media, dielectric function $\epsilon(q,\omega)$, differential inverse mean free path $\tau(E,\omega)$

$$\tau(E,\omega) \sim \int \frac{dq}{q} Im[-\epsilon(q,\omega)^{-1}]$$

$$\Downarrow$$

$$\lambda_{inelast}^{-1} = \int d\omega\, \tau(E,\omega)$$

+ band structure effects: [Ziaja et al.: "Ionization by impact electrons in solids: Electron mean free path fitted over a wide energy range", J. Appl. Phys. 99 (2006) 033514]

Particle approach

Example: MC code for modelling Auger-electron cascade in diamond

Time evolution of the cascade

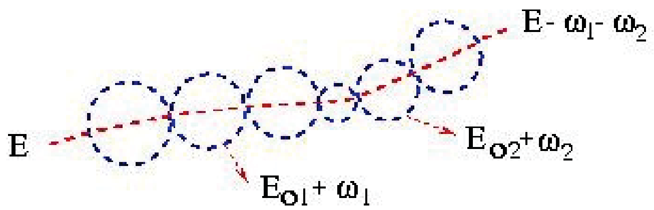

E_{0i} depends on the electronic band structure.

Here: Fermi free-electron band.

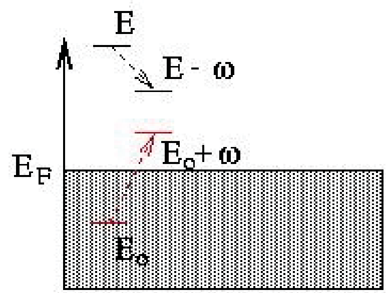

Particle approach

Example: MC code for modelling Auger-electron cascade in diamond

Results: spatio-temporal evolution of electron cascade

Electron range:

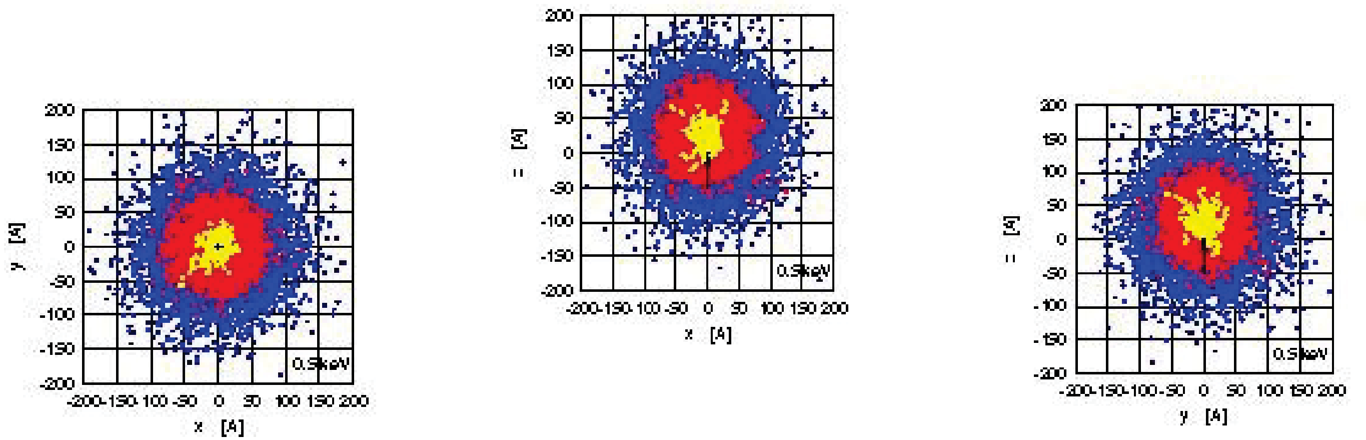

Particle approach

Example: MC code for modelling an Auger-electron cascade in diamond

Results: spatio-temporal characteristics of the cascade

Ionization, $N_{ion}(t)$

Range, $R(t)$

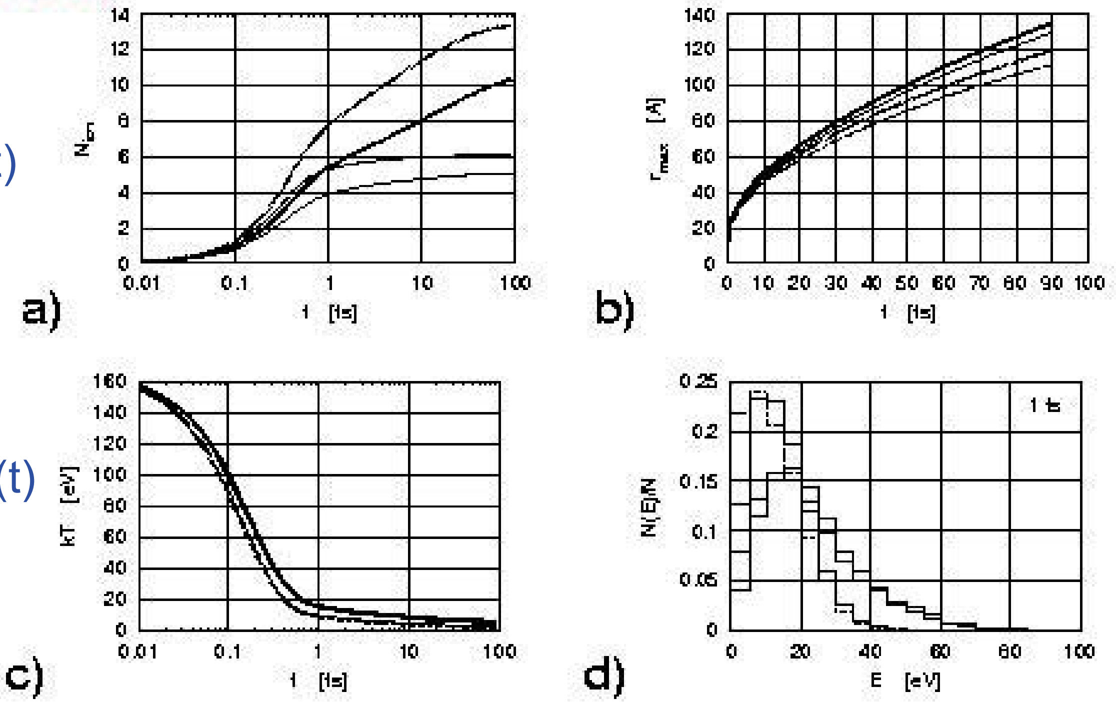

Temperature, $kT(t)$

Energy, $N_{ion}(E)$

Particle approach

Example: MC code to follow electron dynamics within FLASH irradiated aluminum by N. Medvedev and B. Rethfeld.

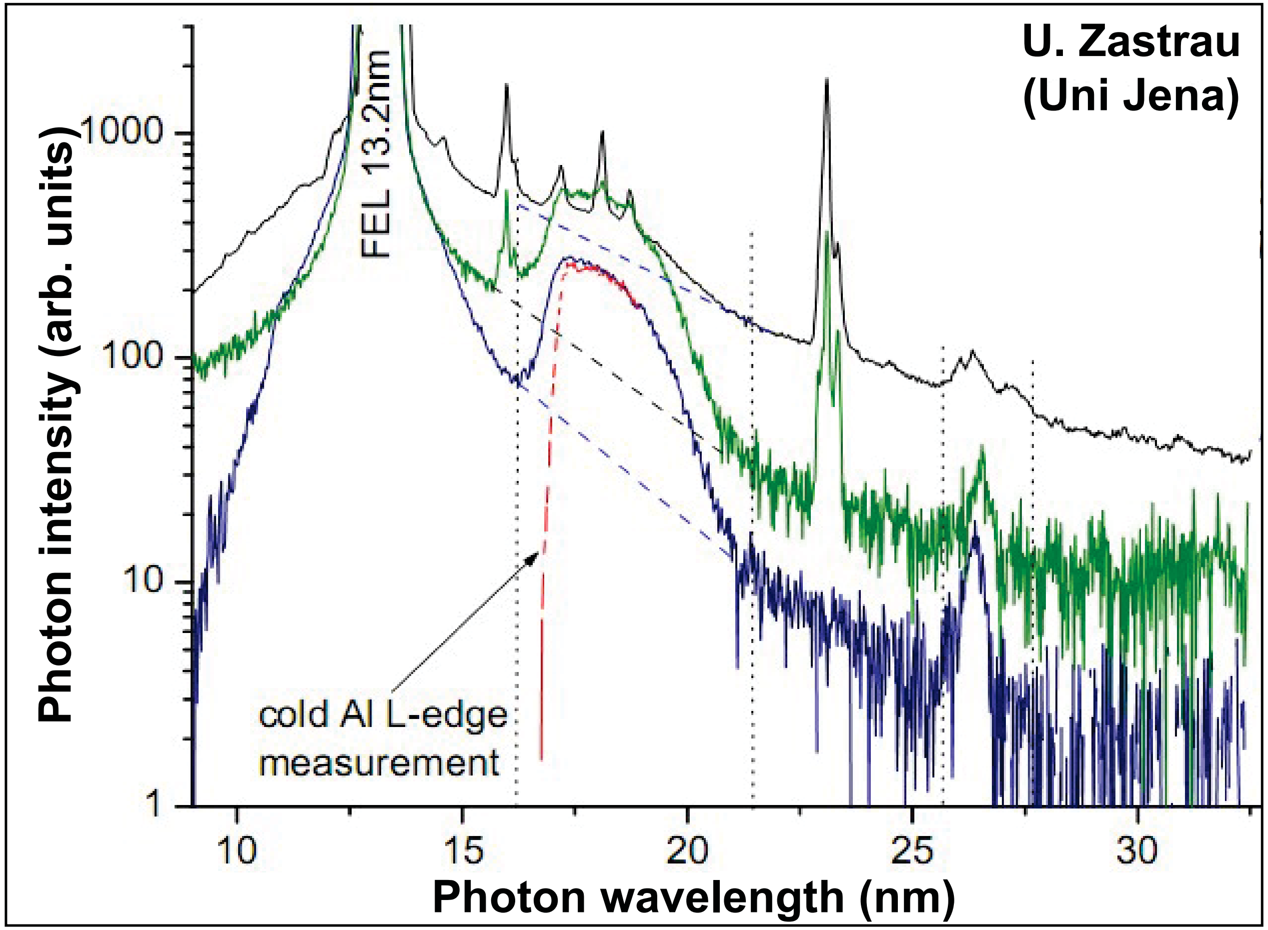

[N. Medvedev,B. Rethfeld PRL 107 (2011)]

Motivation

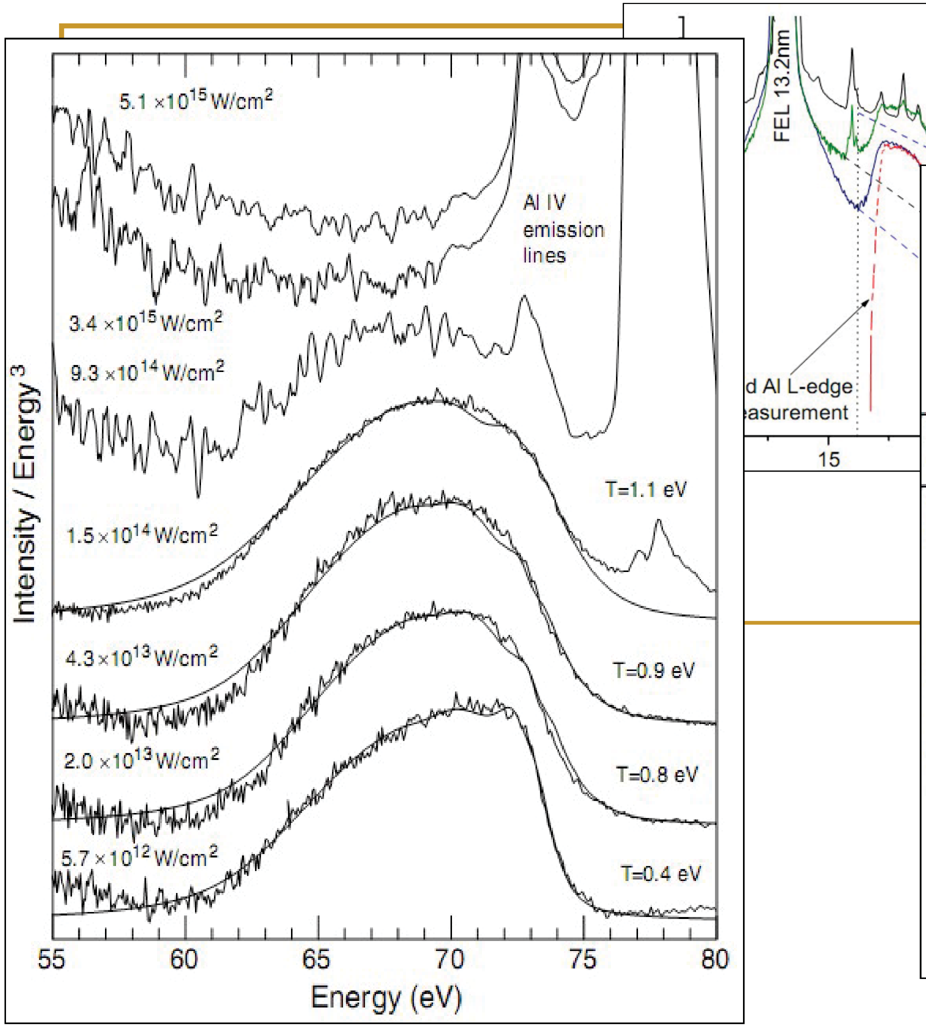

[S. Vinko *et al*, PRL 104, 225001 (2010)]

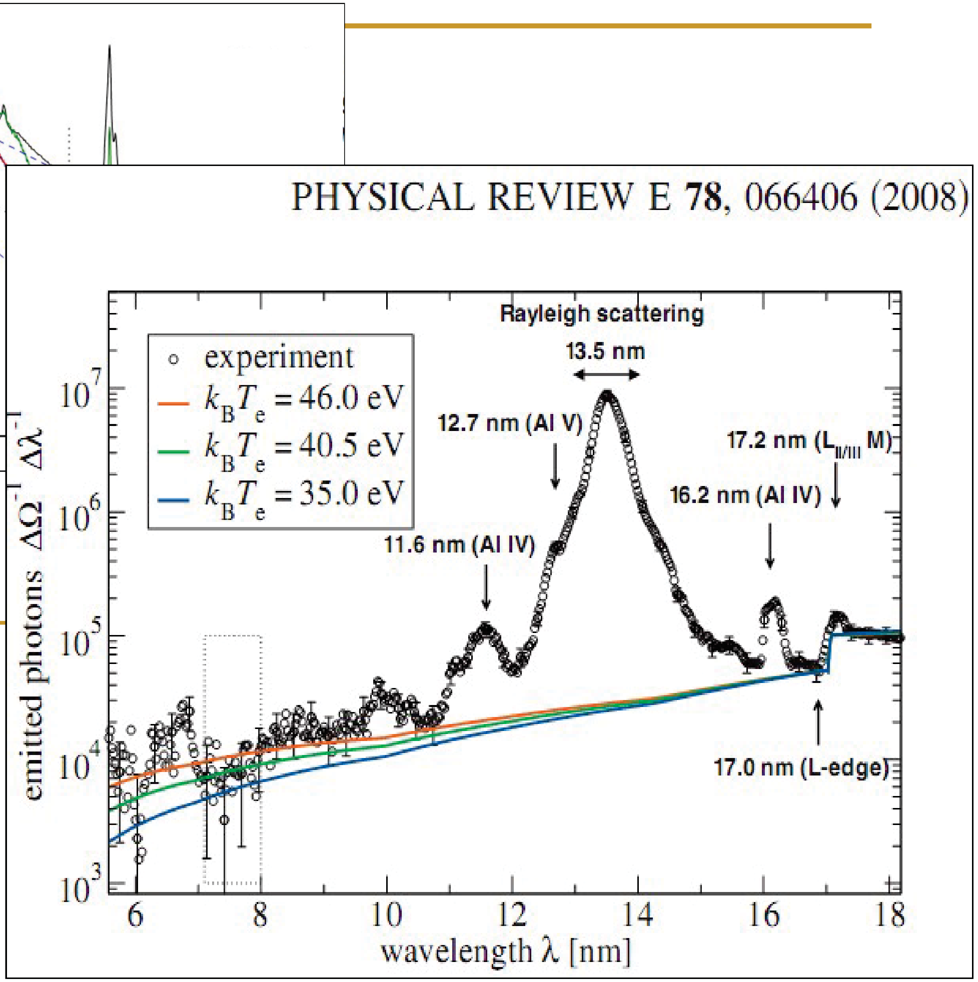

[U. Zastrau *et al*, PRE 78, 066406 (2008)]

T_e ~ 1 eV

T_e ~ 40 eV

Monte-Carlo method

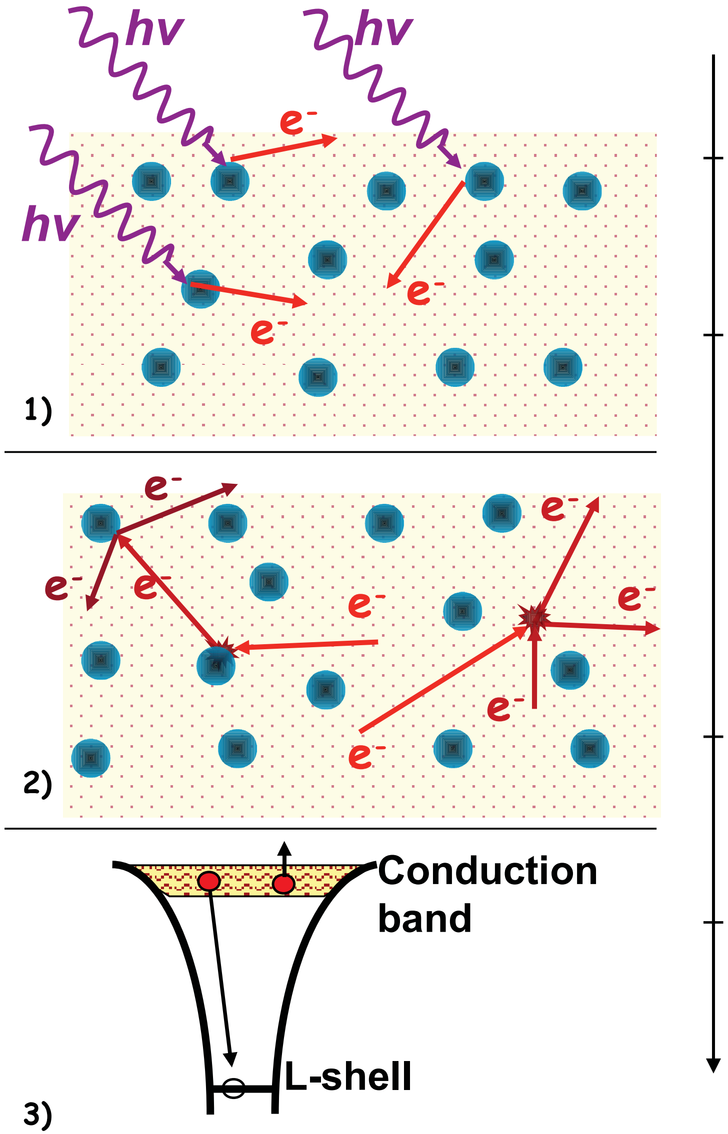

1) Photo-absorption (10 fs, pulse)

2) Electron redistribution:

impact ionizations, elastic scattering, free-electron scattering

3) Auger-like transitions (~ 40 fs)

to deep shells

Ultra short timescales => electronic processes only

[N. Medvedev,B. Rethfeld PRL 107 (2011)]

Qualitative comparison

Influence of different processes: photoabsorption, Auger, scattering

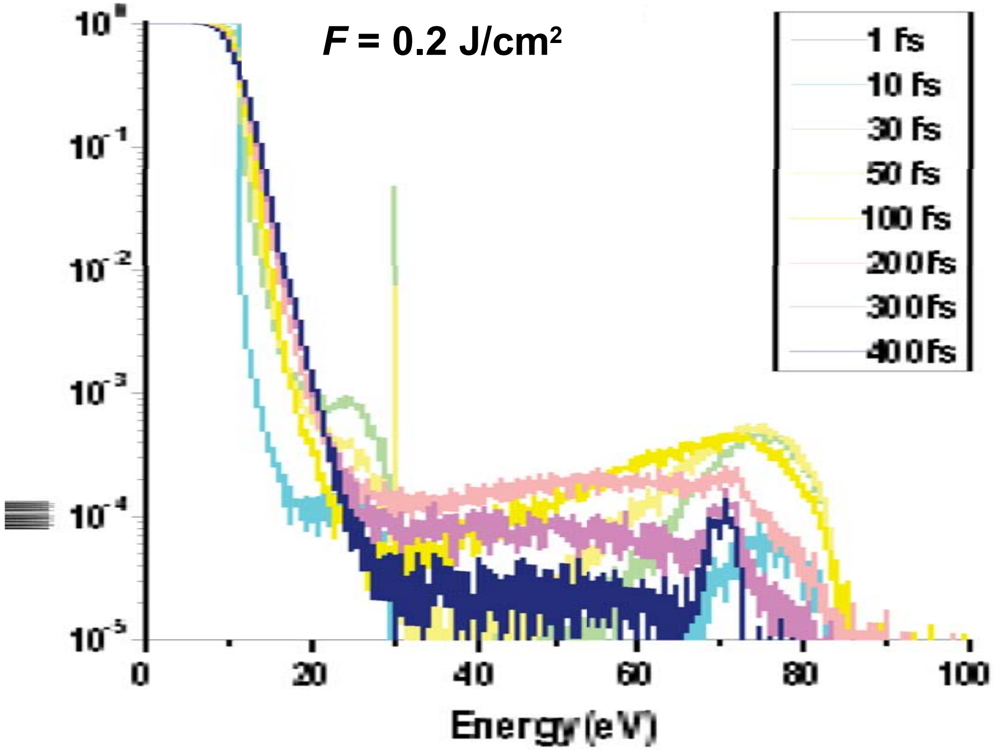

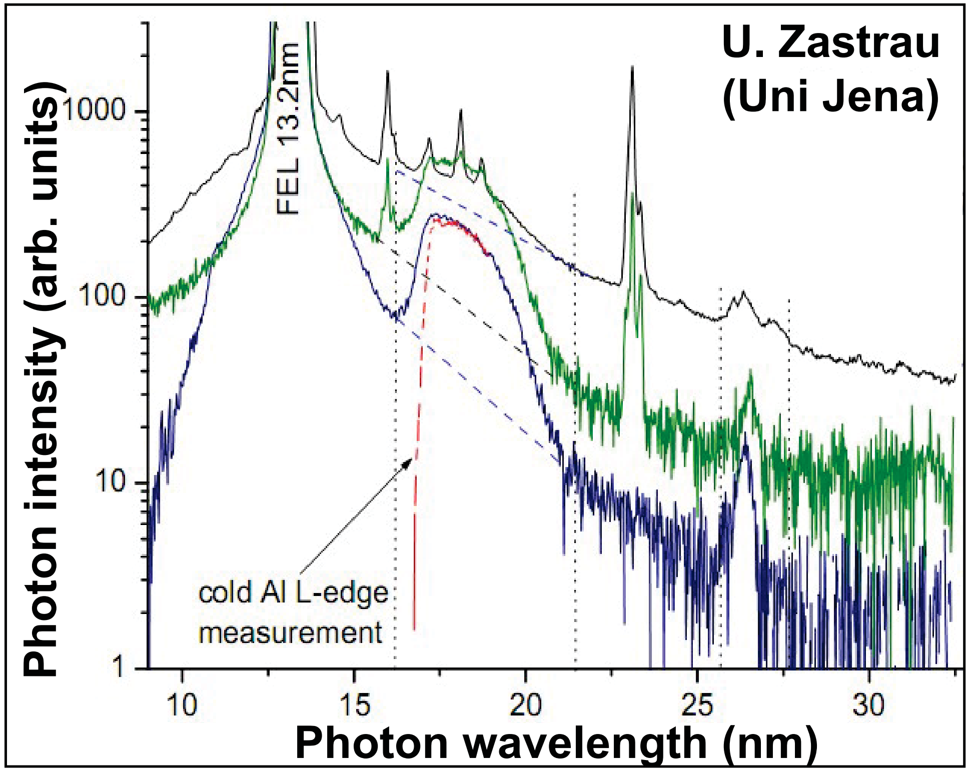

Two parts of distribution:

close to thermalized one + long nonthermalized tail

bump (~1 eV) **background (~20 eV)**

[N. Medvedev, B. Rethfeld PRL 107 (2011)]

Quantitative comparison

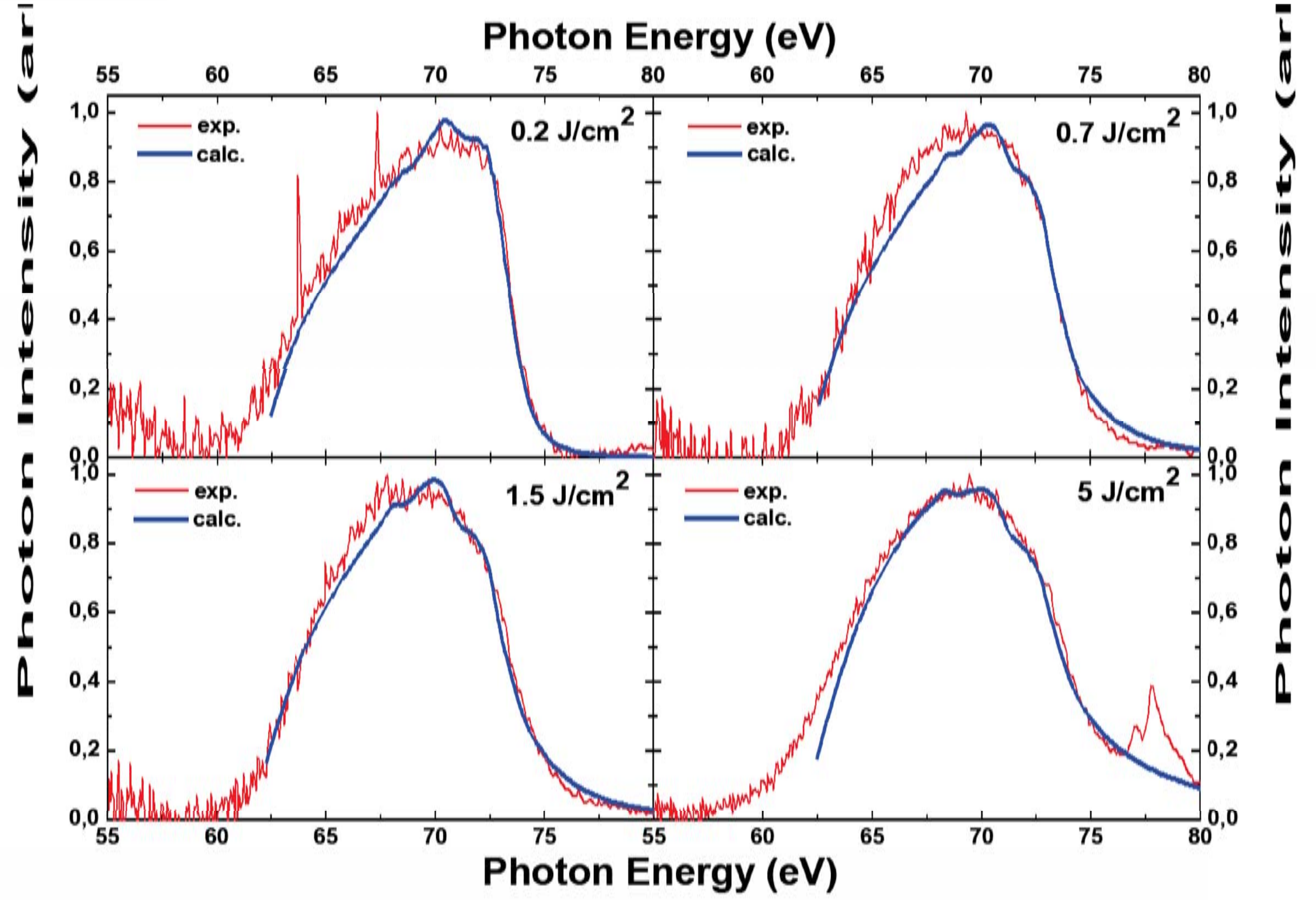

Good agreement with experiment

[N. Medvedev,B. Rethfeld PRL 107 (2011)

Observations

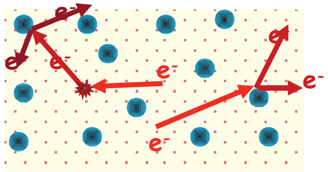

1. Monte-Carlo with electronic band structure

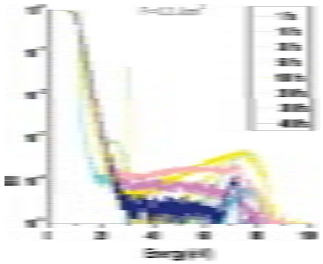

2. Electronic distribution of two parts:
   - Low energetic, close to fermi-distribution
   - High energetic, non-thermalized

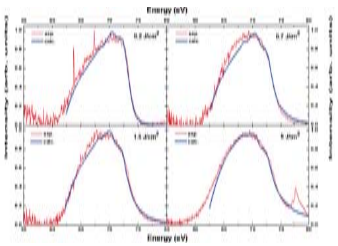

3. Experiments with Auger/radiative-decay spectra reflect only low energy electrons

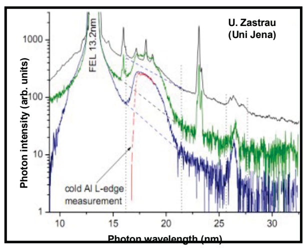

4. Bremsstrahlung spectra have access to high energy tail

[N. Medvedev,B. Rethfeld PRL 107 (2011)]

Transport approach

Statistical description of a classical system in terms of density functions $\rho(\mathbf{r}, \mathbf{v}, t)$ in phase space

$\rho(\mathbf{r}, \mathbf{v}, t) d^3r\, d^3v$ is a number of particles located at $\mathbf{r}$ of velocity $\mathbf{v}$ in the phase space element $d^3r\, d^3v$

$$\int \rho(\mathbf{r}, \mathbf{v}, t) d^3r\, d^3v = N(t)$$

$$\int \rho(\mathbf{r}, \mathbf{v}, t)\, d^3r = n(\mathbf{v}, t)$$

$$\int \rho(\mathbf{r}, \mathbf{v}, t)\, d^3v = n(\mathbf{r}, t)$$

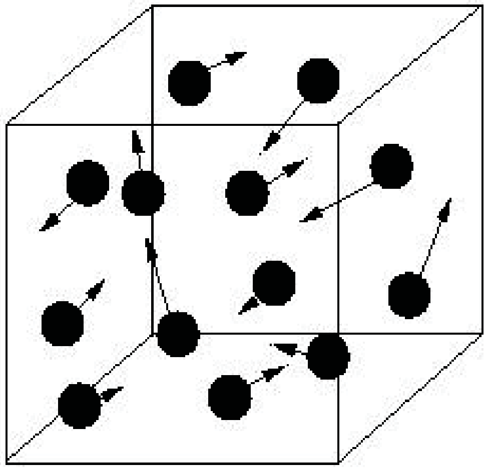

Transport approach

Methods:

- Semiclassical Boltzmann equation
- Hydrodynamic models

Transport approach

Time evolution of the system

$$t \rightarrow t + dt$$

$$\mathbf{r} \rightarrow \mathbf{r} + \mathbf{v}dt$$

$$\mathbf{v} \rightarrow \mathbf{v} + \mathbf{a}dt$$

$$\begin{aligned} \rho(\mathbf{r} + \mathbf{v}dt, \mathbf{v} &+ \mathbf{a}dt, t + dt)d^3r\, d^3v \\ &- \rho(\mathbf{r}, \mathbf{v}, t)d^3r\, d^3v = 0 \end{aligned}$$

Boltzmann equation

$$\partial_t \rho + \mathbf{v}\partial_{\mathbf{r}}\rho + \mathbf{a}\partial_{\mathbf{v}}\rho = 0$$

If there is a collision or a change of particle number:

$$\partial_t \rho + \mathbf{v}\partial_{\mathbf{r}}\rho + \mathbf{a}\partial_{\mathbf{v}}\rho = \Omega(\rho, \mathbf{r}, \mathbf{v}, t),$$

where Ω is a source (collision) term.

Statistical Boltzmann approach

- first-principle approach
- single-run method
- computational costs do not scale with number of atoms

Difficulty:

- requires advanced numerical methods

Boltzmann equations are able to follow

non-equilibrium processes

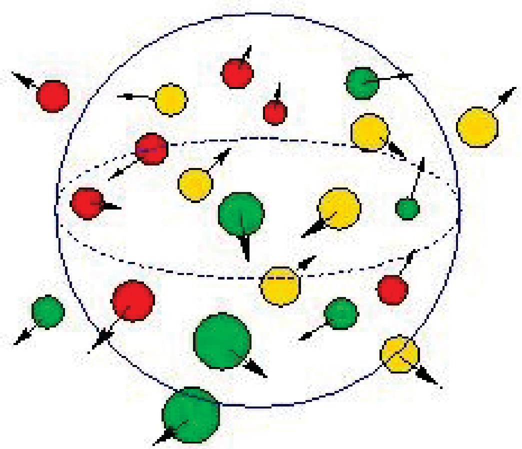

Solving Boltzmann equations

The general coupled Boltzmann equations for electron, $\rho^{(e)}(\mathbf{r},\mathbf{v},t)$, and ion densities, $\rho^{(i)}(\mathbf{r},\mathbf{v},t)$, where $i = 0, 1, \ldots, N_J$ denotes the ion charge, and N_J is the maximal ion charge in the system are:

$$\partial_t \rho^{(e)}(\mathbf{r},\mathbf{v},t) + \mathbf{v}\cdot\partial_{\mathbf{r}}\rho^{(e)}(\mathbf{r},\mathbf{v},t) + \frac{e}{m}\left(\mathbf{E}(\mathbf{r},t) + \mathbf{v}\times\mathbf{B}(\mathbf{r},t)\right)\cdot\partial_{\mathbf{v}}\rho^{(e)}(\mathbf{r},\mathbf{v},t) = \Omega^{(e)}(\rho^{(e)},\rho^{(i)},\mathbf{r},\mathbf{v},t),$$

$$\partial_t \rho^{(i)}(\mathbf{r},\mathbf{v},t) + \mathbf{v}\cdot\partial_{\mathbf{r}}\rho^{(i)}(\mathbf{r},\mathbf{v},t) - \frac{ie}{M}\left(\mathbf{E}(\mathbf{r},t) + \mathbf{v}\times\mathbf{B}(\mathbf{r},t)\right)\cdot\partial_{\mathbf{v}}\rho^{(i)}(\mathbf{r},\mathbf{v},t) = \Omega^{(i)}(\rho^{(e)},\rho^{(i)},\mathbf{r},\mathbf{v},t).$$

These equations include the total electromagnetic force acting on ions and electrons. Collision terms, $\Omega^{(e,i)}$, describe the changes of the electron/ion densities of velocities $(\mathbf{v}, \mathbf{v}+d\mathbf{v})$ measured at the positions $(\mathbf{r}, \mathbf{r}+d\mathbf{r})$ with time. These changes are due to short-range processes, e. g. collisions, photoabsorptions. The number of processes involved in the sample dynamics depends on the radiation wavelength.

Boltzmann solver

Investigates the non-equilibrium phase of evolution of an irradiated sample until thermalization of electrons and saturation of ionization is reached

It uses the angular moment expansion for density function, ρ:

$$\rho \sim \rho_0 + \rho_1 \cdot \cos\theta_{vr} + \rho_2 \cdot \cos\theta_{v\varepsilon}$$

with dominating isotropic component of ρ. This is appropriate for the non-equilibrium phase of sample evolution

Boltzmann solver: accuracy tests

- Flow control in real space → check how many particles and how much energy escaped from the simulation box → accuracy < 5%
- Energy and number of particles conserved with a good accuracy (< 1%) in collisionless case
- Collisionless motion simulated with Boltzmann solver checked with an analytical model
- Accuracy of pseudospectral approximation checked with an independent method

Four spheres of flow control

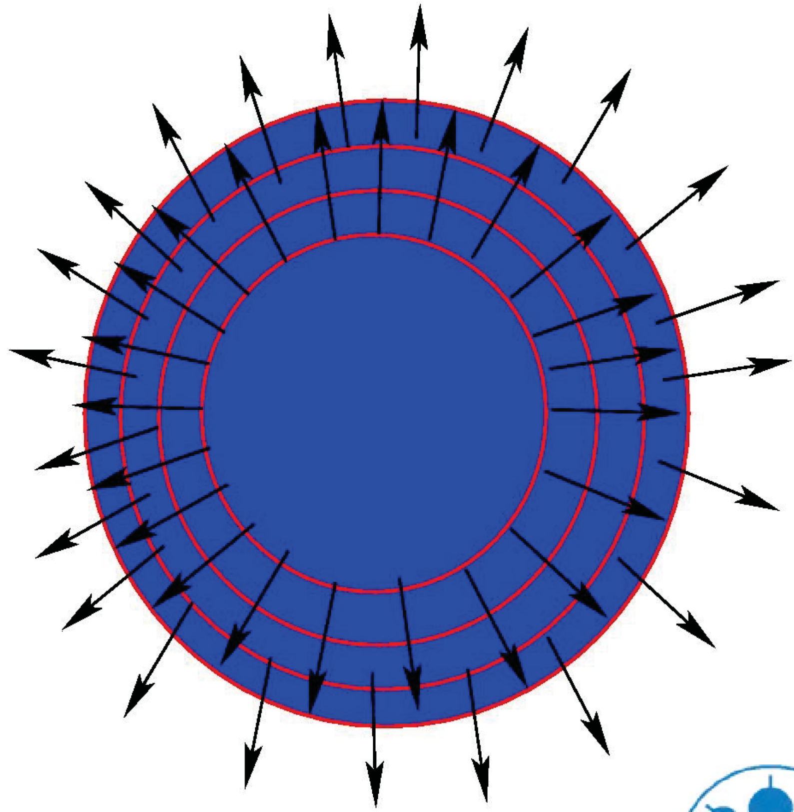

Time of flight mass spectra of Xe atoms and clusters at radiation wavelength 100 nm

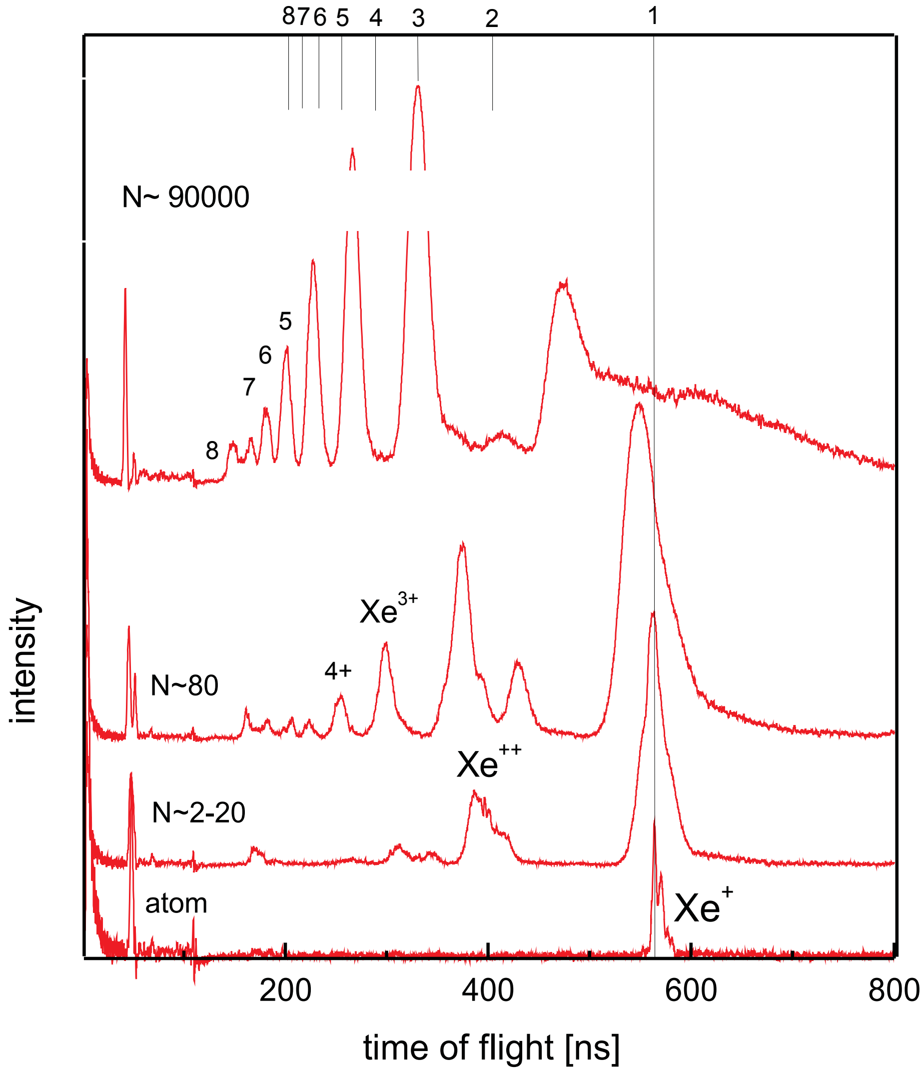

10^{12}-10^{14} W/cm^2

[H. Wabnitz et al, Nature 420, 482 (2002)]

Ip_{Xe} = 12.1 eV
E_{phot} = 12.8 eV

- **Multiply charged ions from clusters, keV energy**
- **Only singly charged ions from atoms**

↓↓

Dedicated theoretical study needed to explain the enhanced energy absorption

pulse duration ~ 50 fs

Theoretical models proposed

- Enhanced inverse bremsstrahlung heating of quasi-free electrons within the cluster [Santra, Greene]. Enhanced heating rate obtained with effective atomic potential. High charge states produced during collisional ionizations **[R. Santra, Ch. H. Green, PRL 91, 233401 (2003)]**
- High charge states within clusters are produced by single photon absorptions due to the suppression of the interatomic potential barriers within the cluster environment [Georgescu, Saalmann, Siedschlag, Rost] **[C. Siedschlag, J. M. Rost , PRL 93, 43402 (2004)]**
- Heating of quasi-free electrons through many-body recombination [Jungreuthmayer, Ramunno, Zanghellini, Brabec]. High charge states produced during collisional ionizations.

[C. Jungreuthmayer et al. , J. Phys. B 38, 3029 (2005)]

Theoretical modelling

What happens if all enhancement factors are included in one model?

- Creation of high charges through: photoionizations → IB heating of quasi-free electrons as proposed by Santra & Greene → collisional ionizations / recombinations;
- Modification of atomic potentials by electron screening and ion environment tested
- Plasma regime tested → possible contribution of many-body effects (many-body recombination)

↑↑↑↑

- Independent cross-check with MD simulation successful [F.Wang]

Clusters of 2500 xenon atoms irradiated with 100nm FEL pulses of various energies

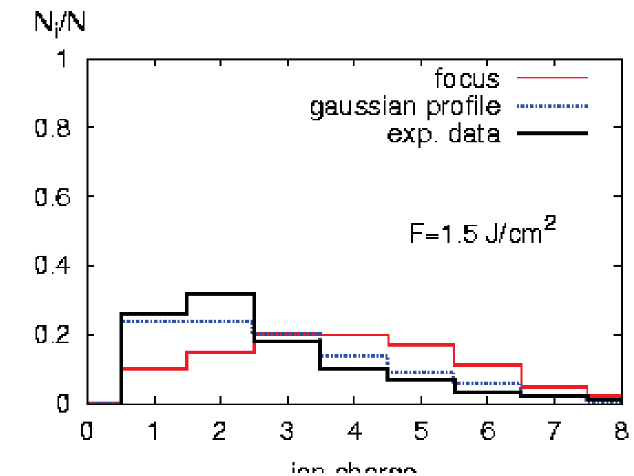

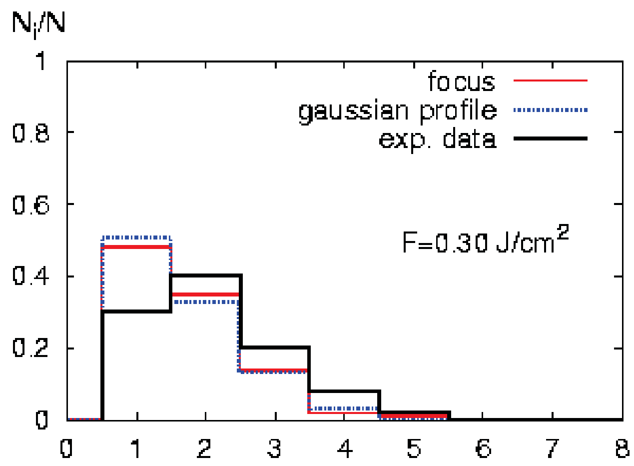

Ion fractions at various pulse fluences

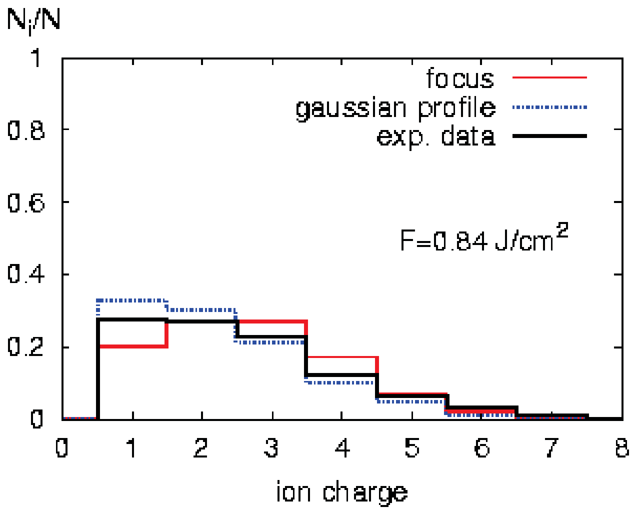

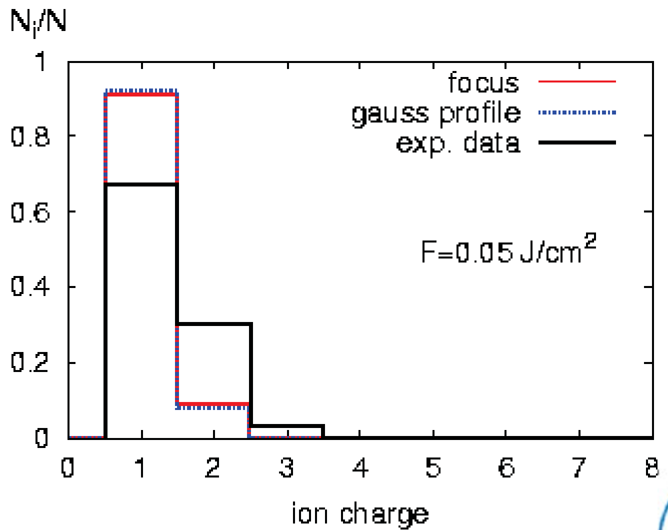

TOF detects only ions !

[Ziaja et al., Phys. Rev. Lett. 102 (2009) 205002]

Clusters of various size irradiated with 100nm FEL pulses of a fixed flux, F=0.4 J/cm²

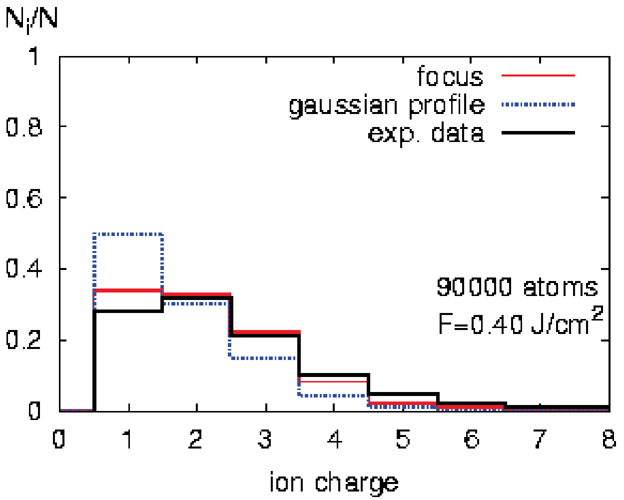

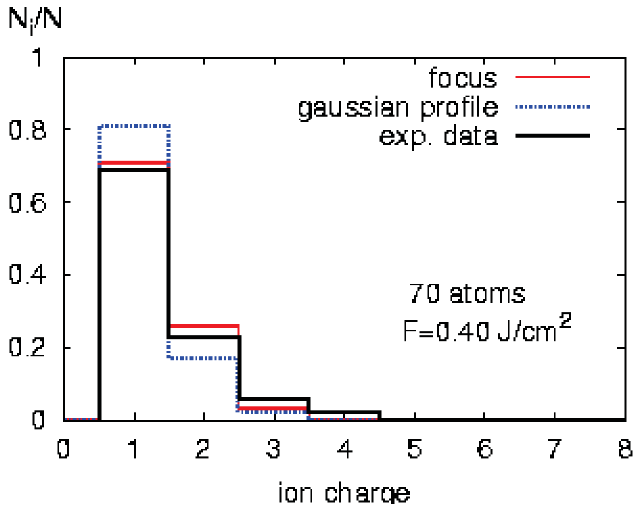

Ion fractions at various cluster size

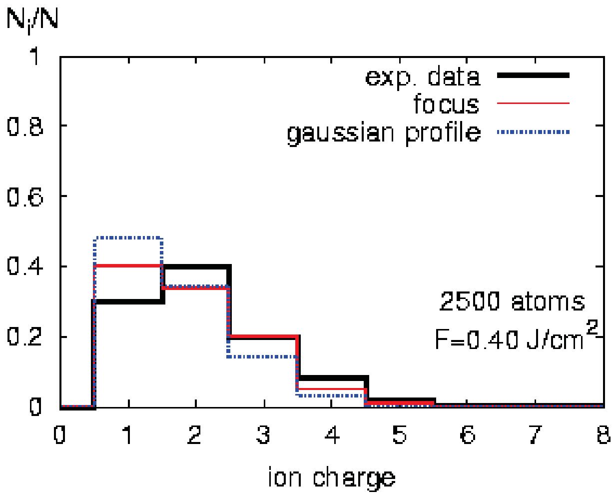

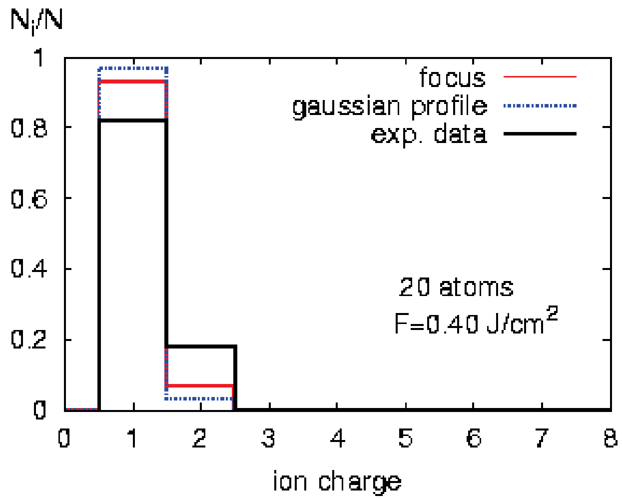

TOF detects only ions !

Electron spectroscopy at 100 nm: indication of energy absorption mechanisms

Electron emission spectra at 100 nm for Xe (70) and Ar (300):

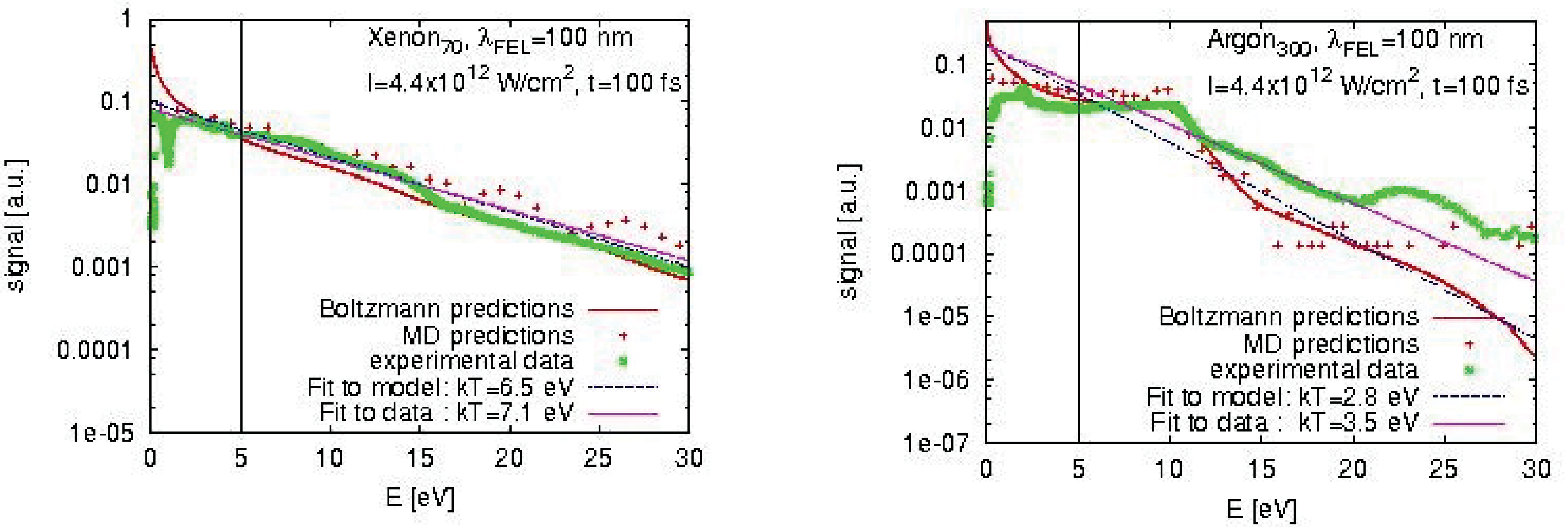

Plasma formation, intense heating of quasi-free electrons

[Ziaja et al., New J. Phys. 11 (2009) 103012]

DESY

Electron spectroscopy at 32 nm: indication of energy absorption mechanisms

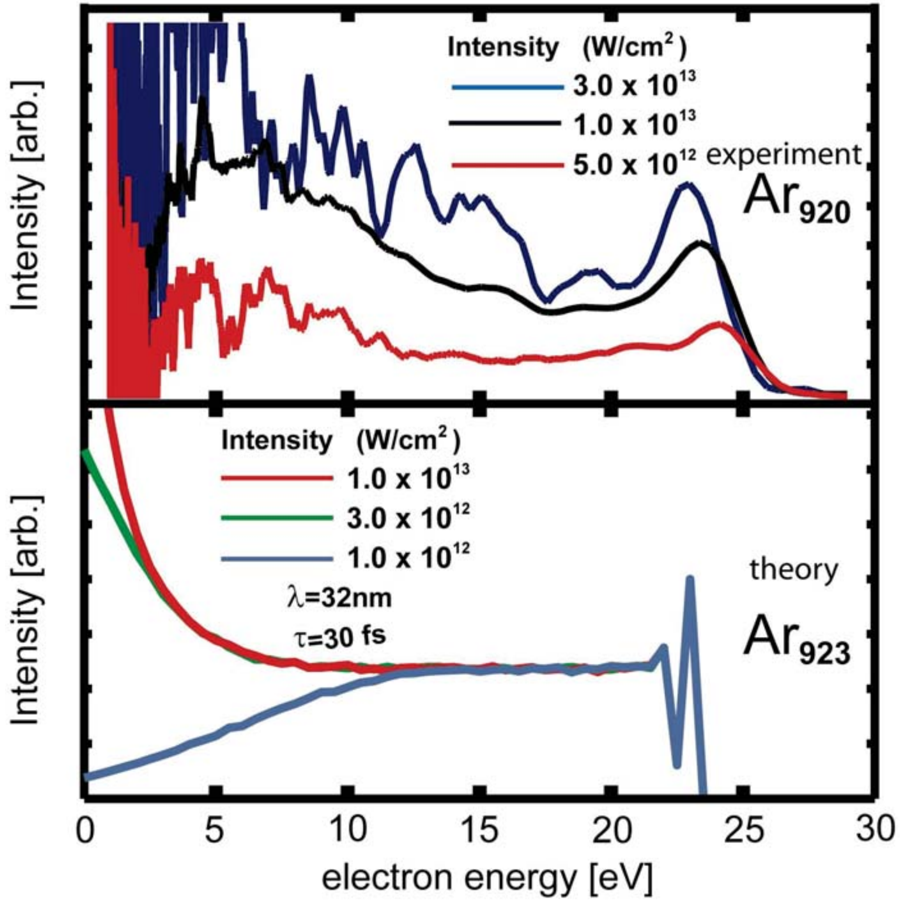

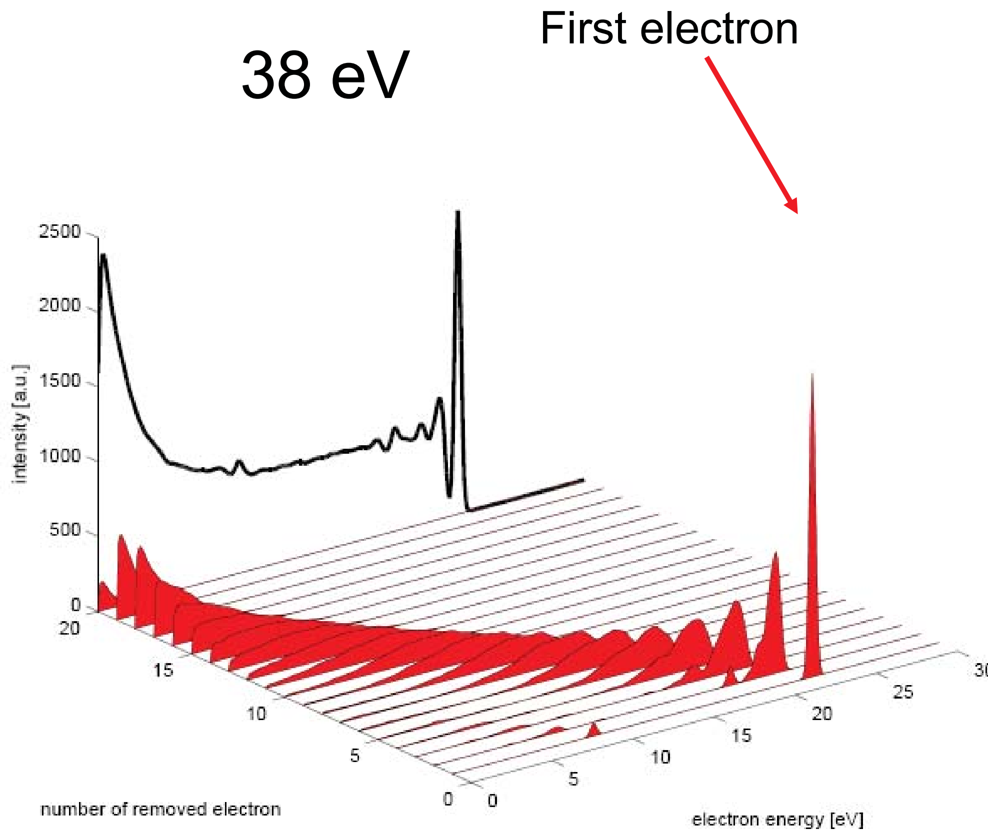

no thermionic electron emission
no plasma absorption [T. Fennel et al.]

[C. Bostedt et al. Phys. Rev. Letters 100, 133401 (2008)]

Electron spectroscopy at 32 nm
indication of energy absorption mechanisms

Electron emission spectra at 32 nm for Ar(80) and Ar (150):
sequential ionization
[Ziaja et al., New J. Phys. 11 (2009) 103012]

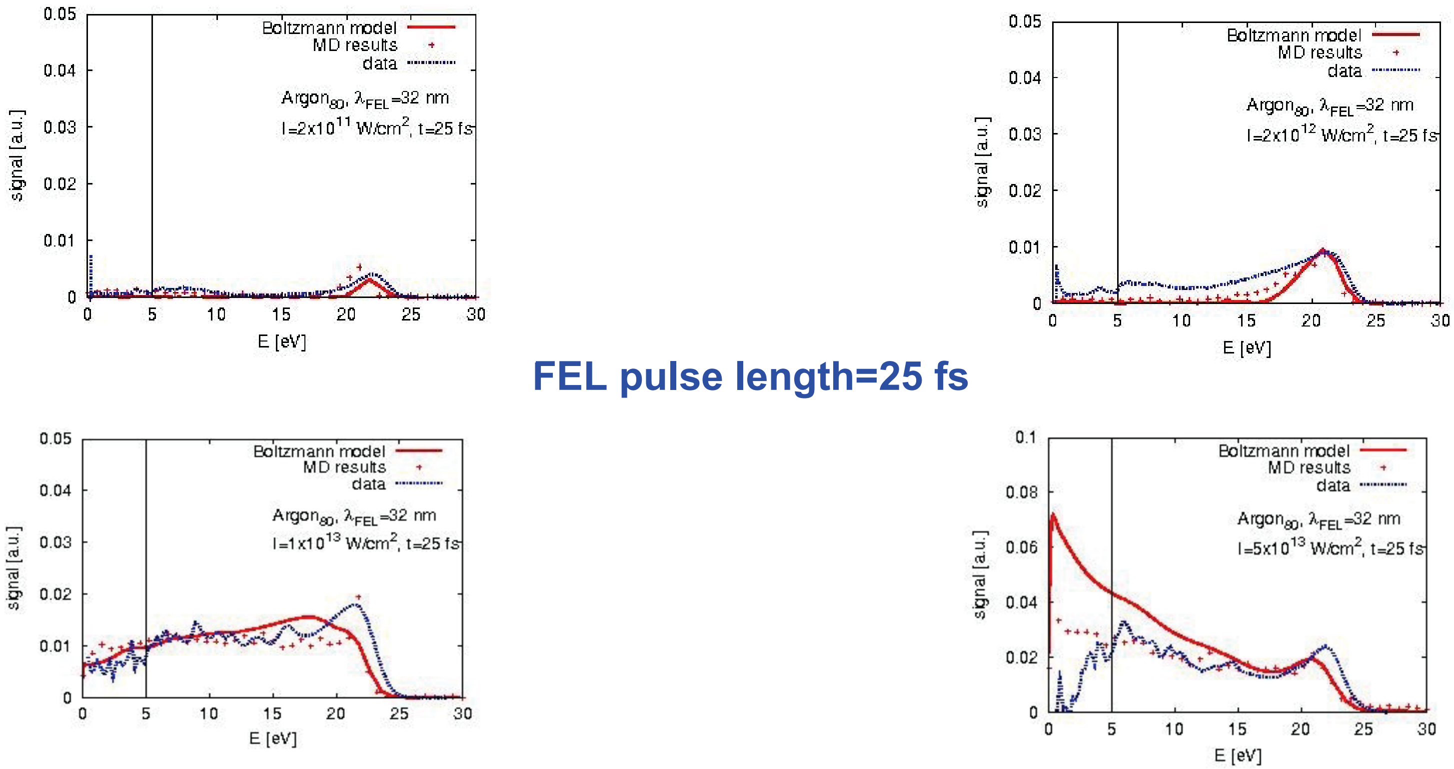

Good agreement of the results with MD simulations by the Rostock group [T. Fennel et al.] and in-house MD simulations [F. Wang]

Soft X-Ray Thomson Scattering in Warm Dense Hydrogen at 13 nm

R.R. Fäustlin, S. Toleikis et al.

[Phys. Rev. Lett. 104 (2010), 125002]

10/01/09, Rostock

We validate impact ionization models

- Liebermann: classical e-e collisions
- BEB includes atomic structure

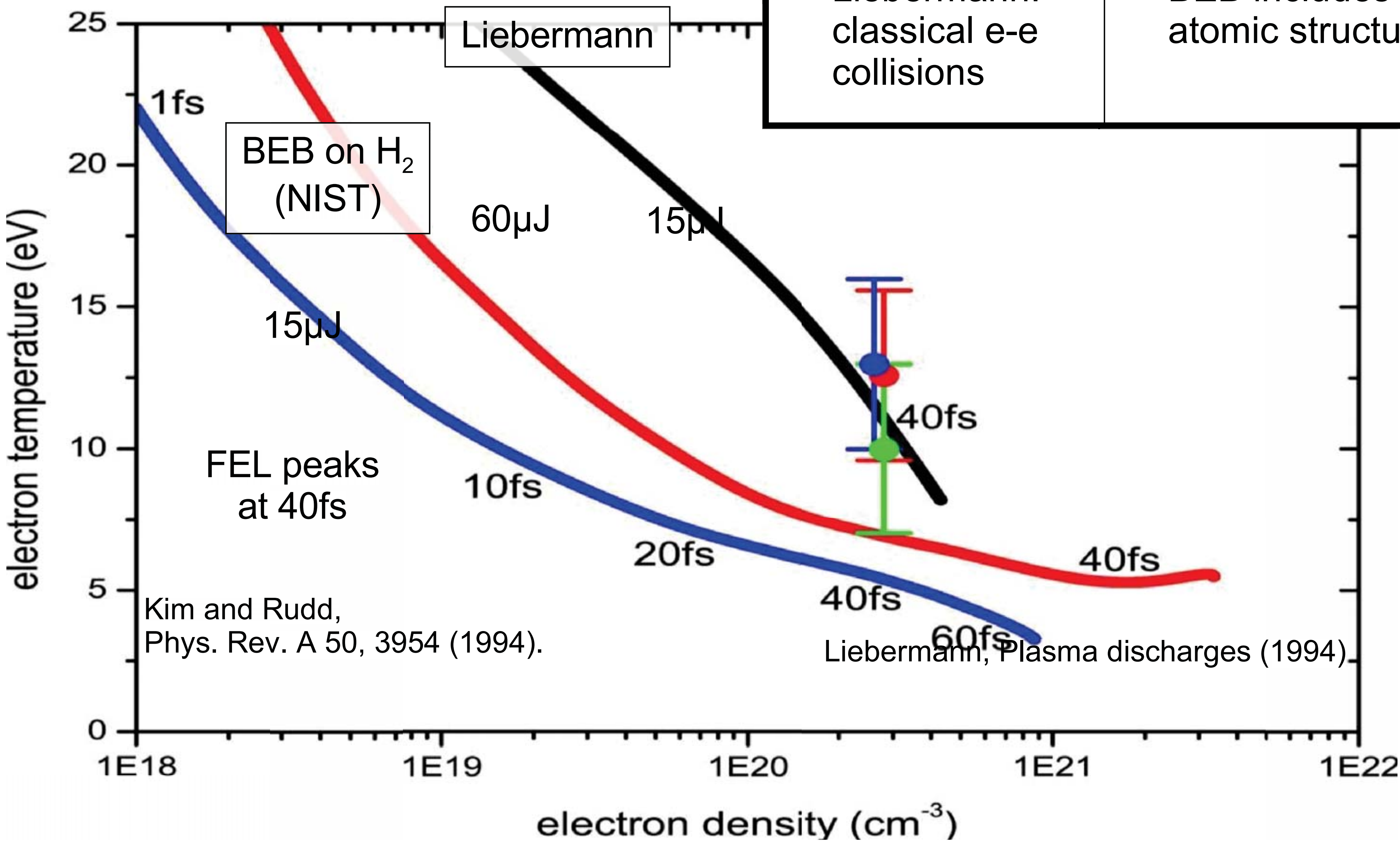

Simulations performed for clusters consisting of 0.5 million atoms

STS probes fs electron thermalization

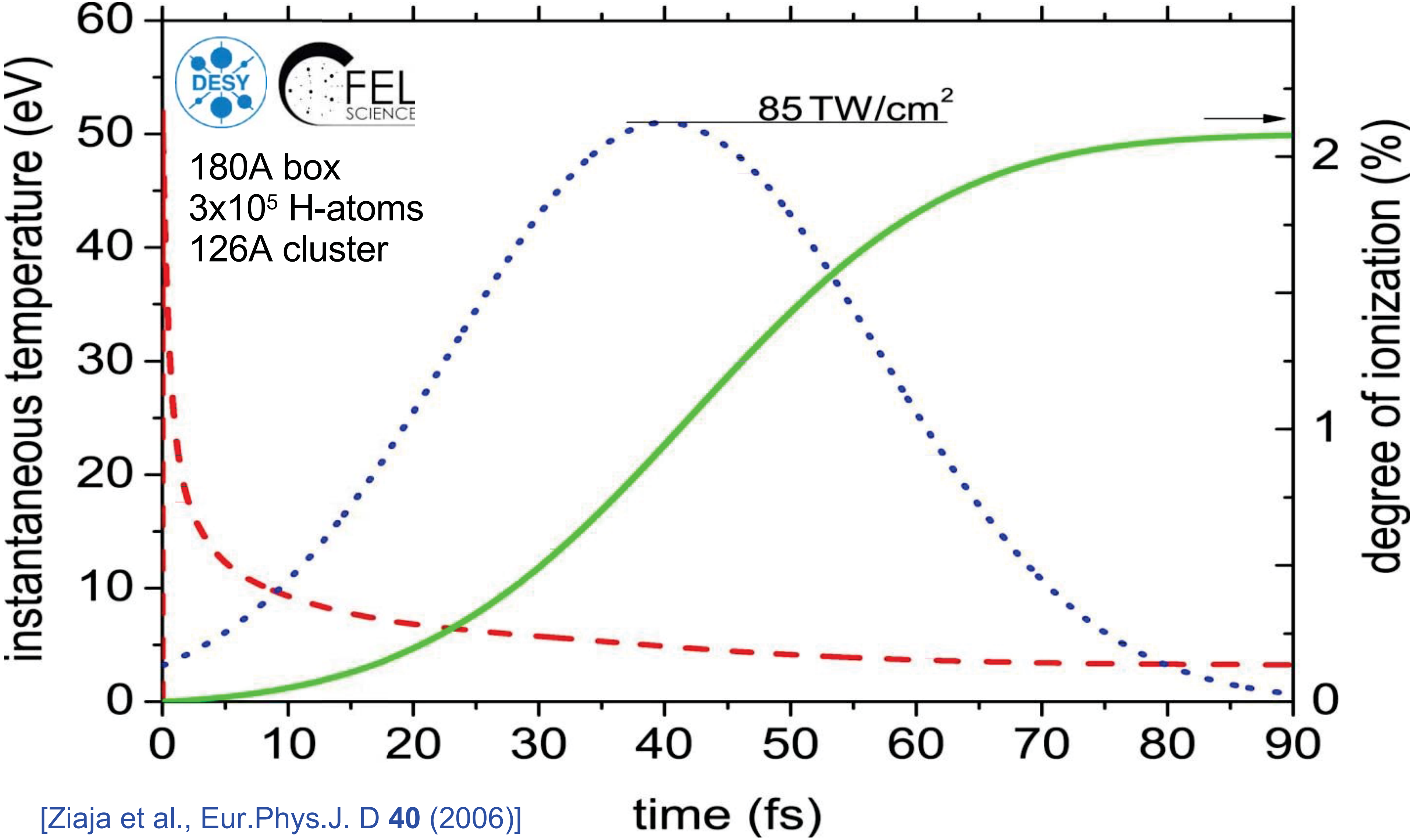

[Ziaja et al., Eur.Phys.J. D **40** (2006)]

Single shot scattering and imaging of large noble gas clusters at wavelength ~ 13 nm

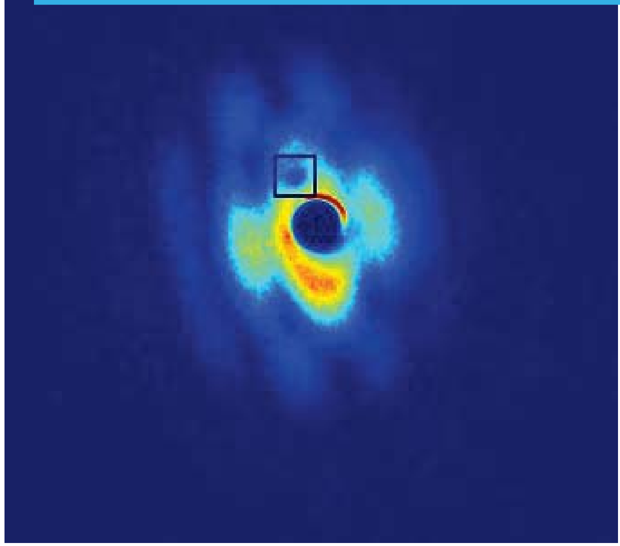

[C. Bostedt, H. Chapman, F. Wang and T. Möller]

scattering pattern

Wavelength 13.7 nm

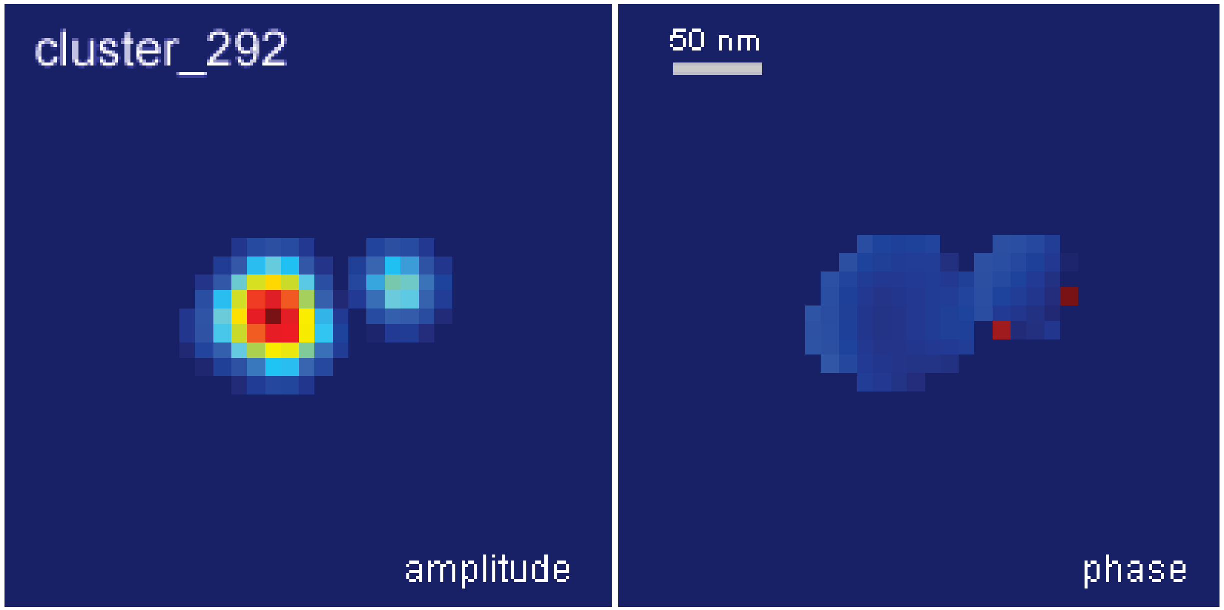

reconstructed image

two clusters in
direct contact

Single shot scattering and imaging of large clusters: reconstruction

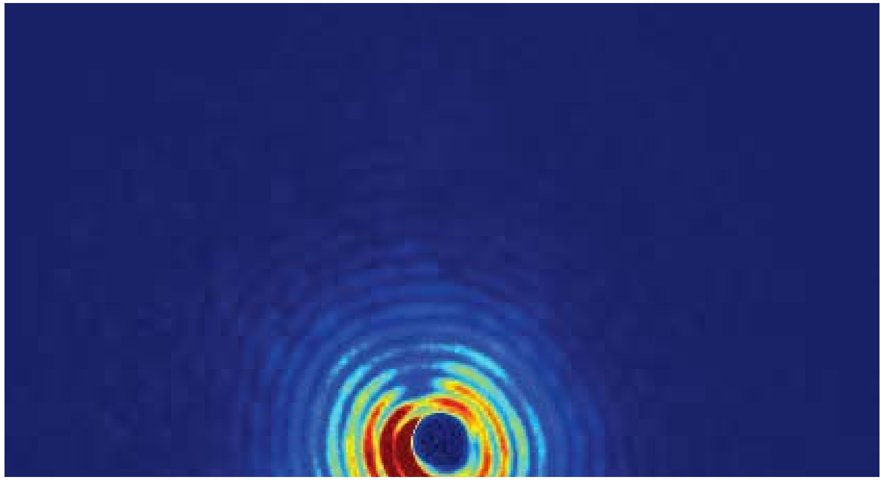

scattering pattern

Wavelength 13.7 nm

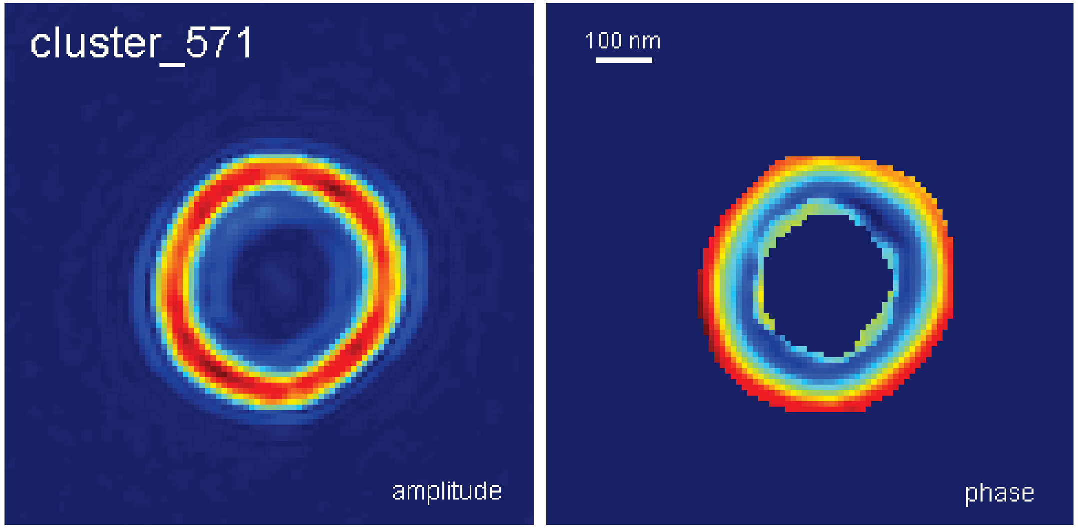

reconstructed image

Delayed ionization and expansion through tampering.

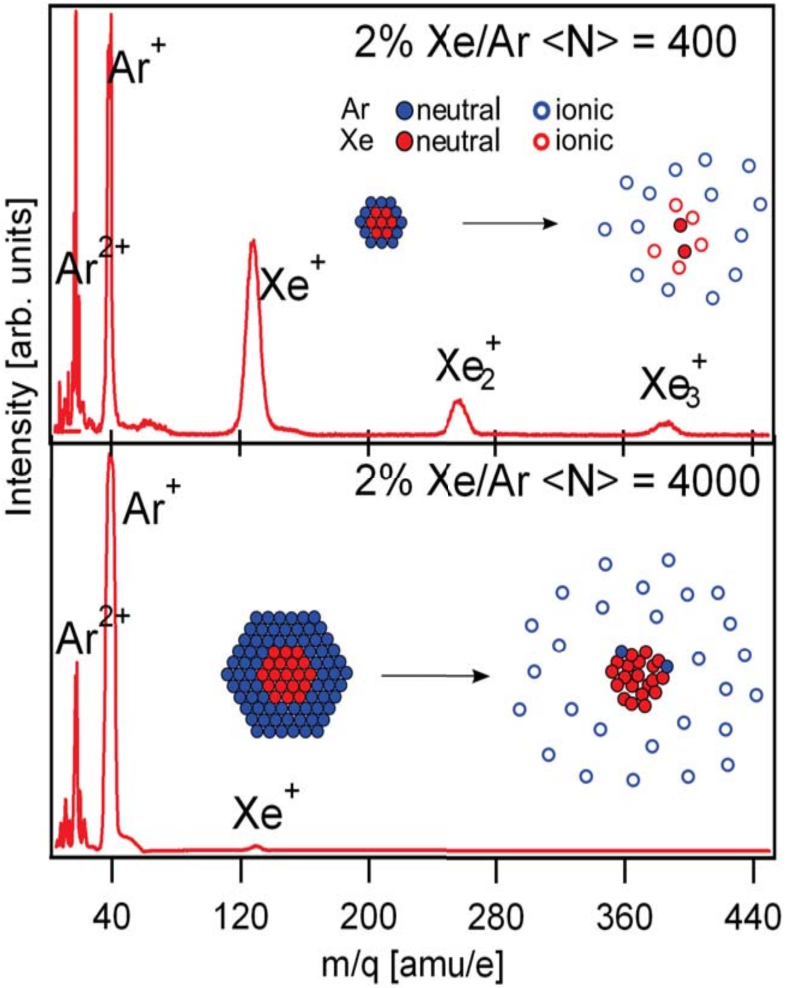

Experiment:
13 nm/ 92 eV, 10^{14} W/cm^2

- **singly charged Ar ions from the surface**
- **strong size effect**
- **Xe plasma in the interior recombines, neutral atoms?**
- **delayed cluster expansion**

M. Hoener,et al J. Phys. B 41, 181001 (2008)

Increased/decreased ionization in mixed Xe/Ar clusters at 32 nm: theory

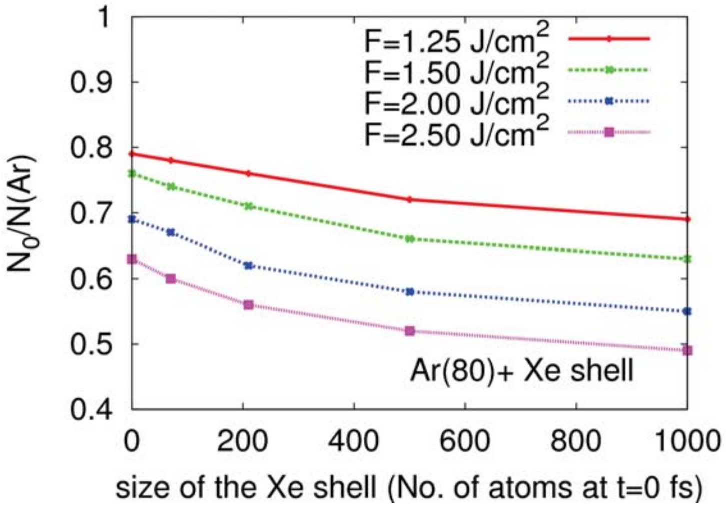

32 nm/ 40 eV, 10^{13} W/cm^2

- **Increased core ionization for Ar/Xe**

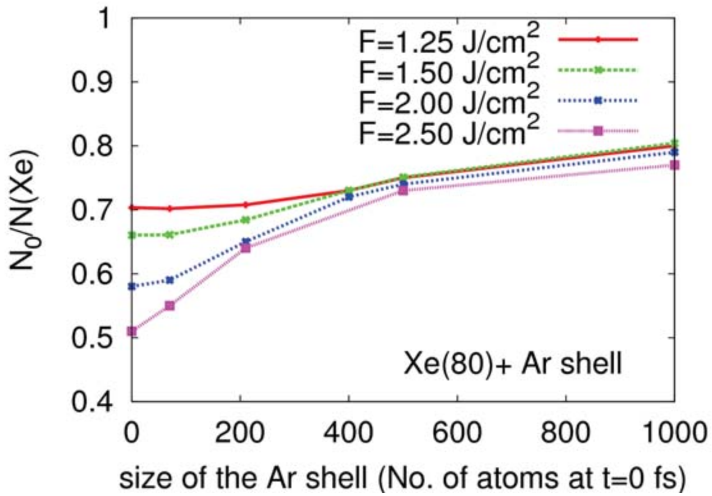

- **Decreased core ionization for Xe/Ar**

Increased/decreased ionization in mixed Xe/Ar clusters at 32 nm: theory

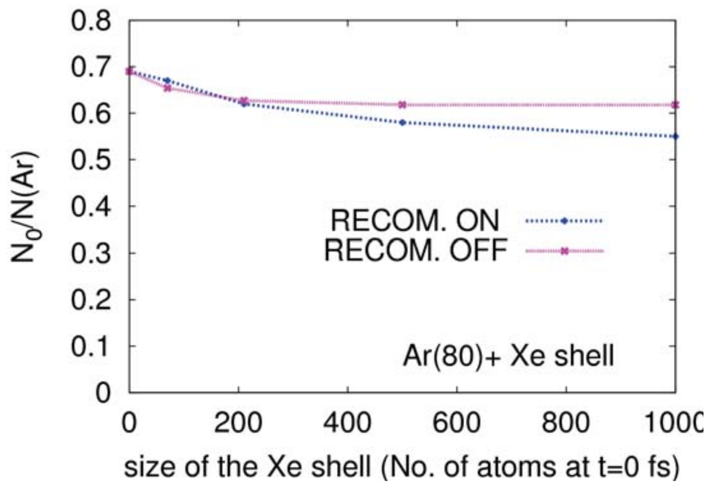

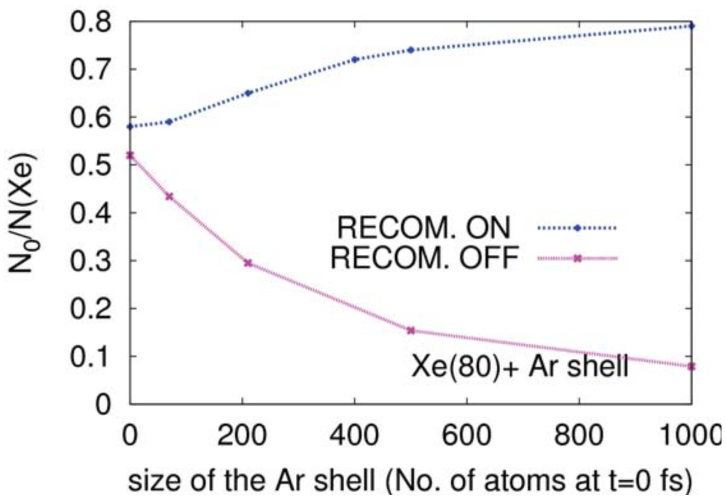

Explanation: three-body recombination

↓

Consequences for single particle imaging

DESY

Combined modular MD/MC/TB/Boltzmann approach to study structural changes in solids

- MD to describe dynamics of ions and atoms
- Boltzmann approach to describe the dynamics of electrons within the valence and conduction bands
- Tight binding method/DFT to describe changes of band structure, potential energy surface
- MC approach to describe dynamics of high energy free electrons in conduction band and creation and relaxation of core holes
- Scattering/ionization rates calculated from complex dielectric function updated at each time step

[N. Medvedev, H. Jeschke, B. Ziaja]

Next 15 slides: courtesy of Nikita Medvedev.

Combined modular MD/MC/TB/Boltzmann approach to study structural changes in solids

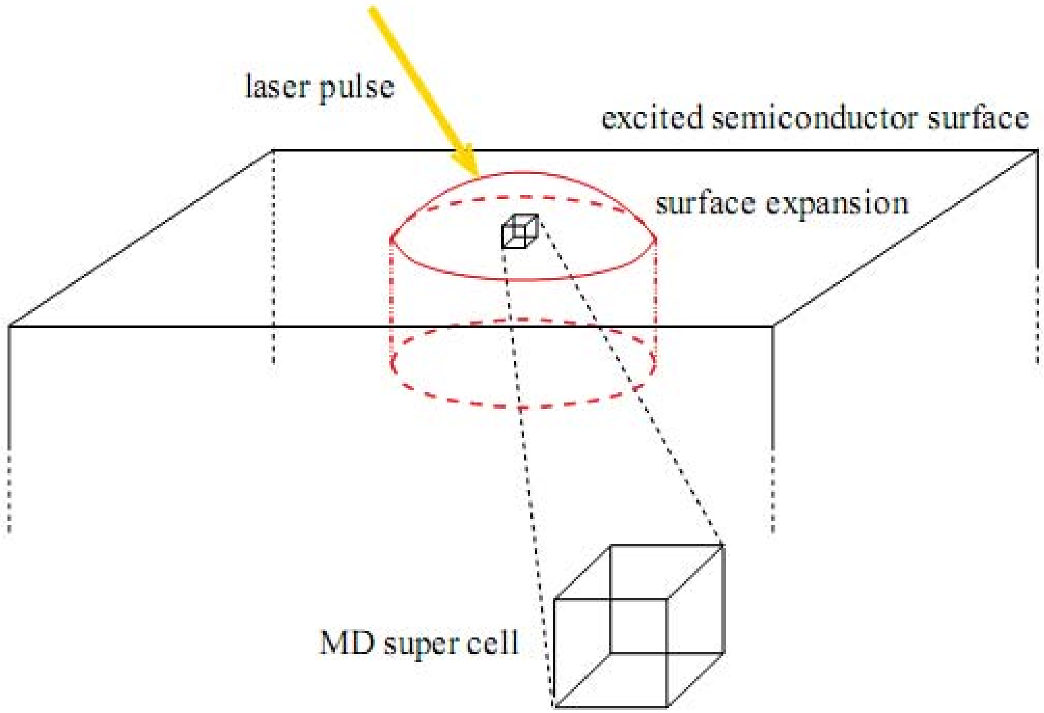

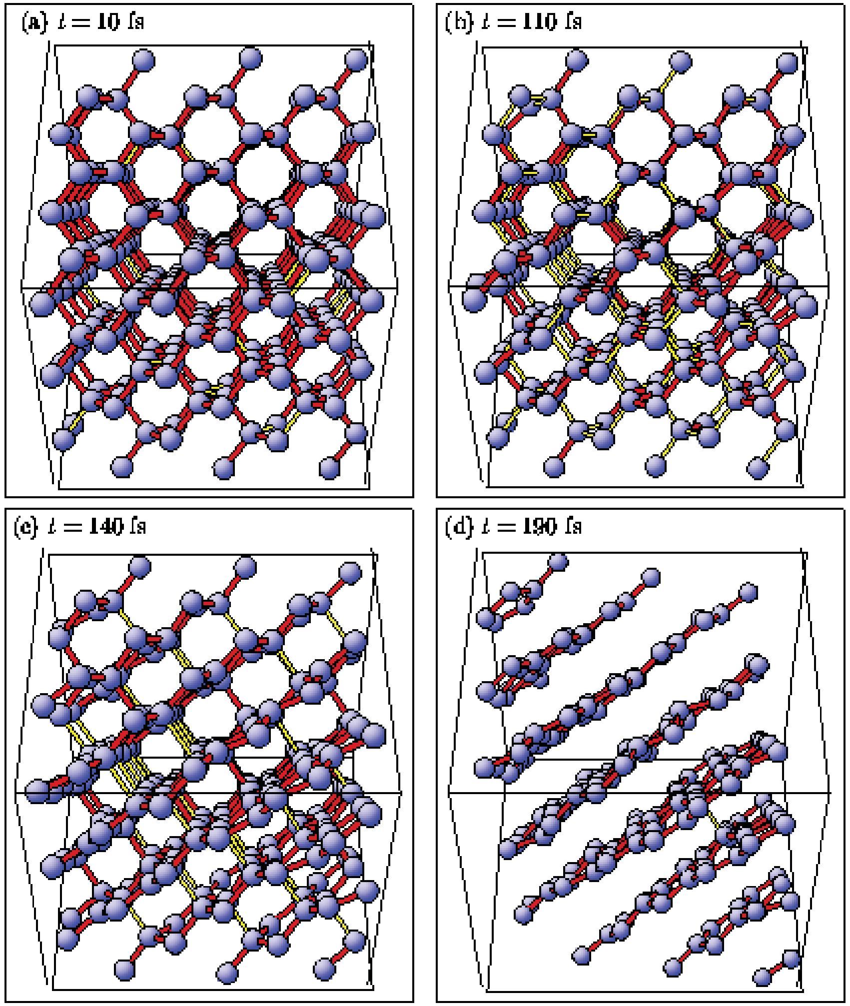

[H. Jeschke et al. PRL 2002]

MD: Equations of motion

$$L = \sum_{i=1}^{N} \frac{m_i}{2} \dot{\mathbf{r}}_i^T \dot{\mathbf{r}}_i - \Phi(\{r_{ij}\}, t) \qquad \frac{d}{dt}\frac{\partial L}{\partial \dot{\mathbf{r}}_k} - \frac{\partial L}{\partial \mathbf{r}_k} = 0 \quad \text{with} \quad k \in \{1, \ldots, N\}$$

$$m_k \ddot{\mathbf{r}}_k = -\frac{\partial \Phi(\{r_{ij}\}, t)}{\partial \mathbf{r}_k}$$

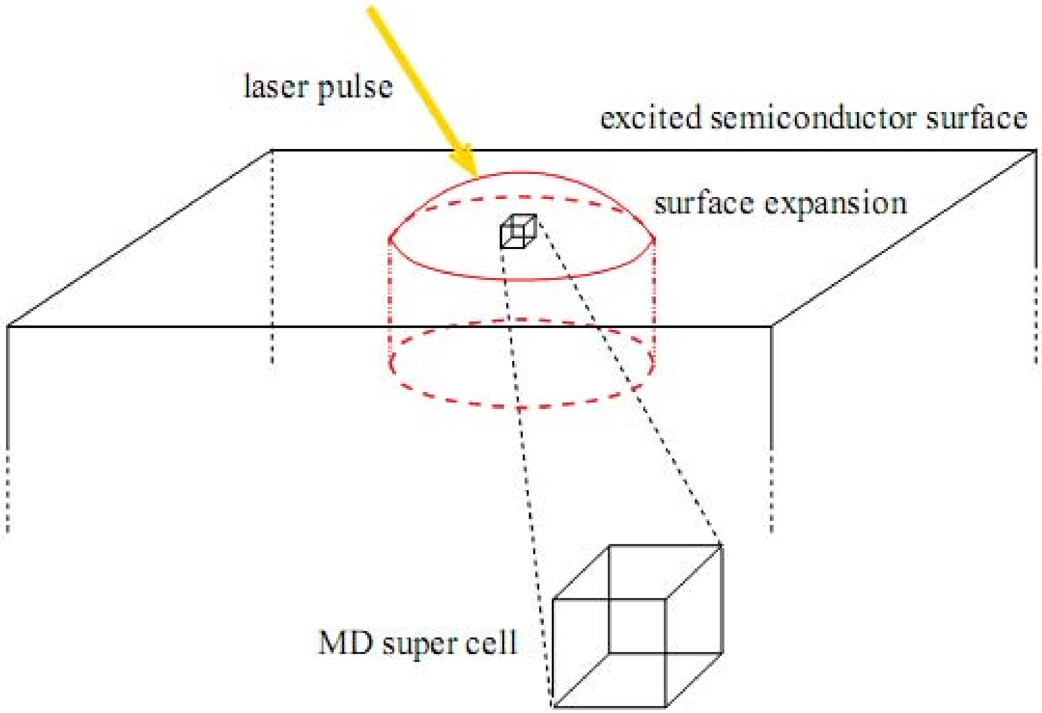

Laser spot ~ 10 micron

> 10^9 atoms

TBMD: 1000 atoms

=> Periodic boundary conditions

MD: Periodic boundary conditions

1) Atoms are locked in the super-cell

2) Interaction between atoms in the super cell + in all images

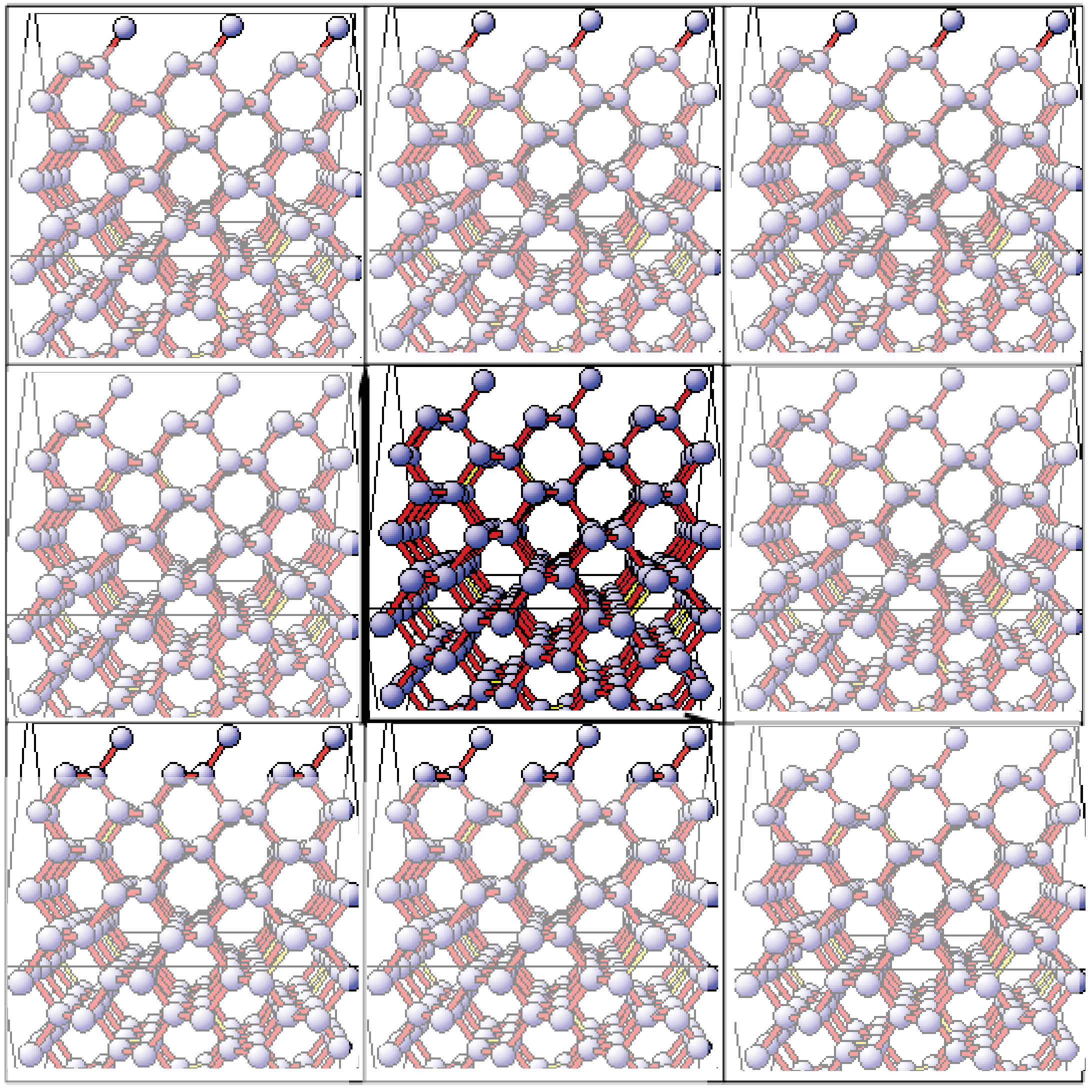

MD: Parrinello - Rahman method

$$L = \sum_{i=1}^{N} \frac{m_i}{2} \dot{\mathbf{s}}_i^{\mathrm{T}} h^{\mathrm{T}} h \, \dot{\mathbf{s}}_i + K_{\mathrm{cell}} - \Phi(\{r_{ij}\}, t) - U_{\mathrm{cell}}$$

$$K_{\mathrm{PR}} = \frac{w_{\mathrm{PR}}}{2} \mathrm{Tr}(\dot{h}^{\mathrm{T}} \dot{h})$$

$$U_{\mathrm{cell}} = p_{\mathrm{ext}} \Omega$$

$$\Omega = \det(h)$$

$$\ddot{\mathbf{s}}_i = -\frac{1}{m_i} \sum_{j \neq i} \frac{\partial \Phi(r_{ij})}{\partial r_{ij}} \frac{\mathbf{s}_i - \mathbf{s}_j}{r_{ij}} - g^{-1} \dot{g} \dot{\mathbf{s}}_i$$

$$\ddot{h} = (\Pi - p_{\mathrm{ext}}) \frac{\sigma}{w_{\mathrm{PR}}}$$

$$\Pi = \frac{1}{\Omega} \sum_{i=1}^{N} m_i \mathbf{v}_i \mathbf{v}_i^{\mathrm{T}} - \frac{1}{\Omega} \sum_{i=1}^{N} \sum_{j>i} \frac{\partial \Phi(\{r_{ij}\}, t)}{\partial r_{ij}} \frac{\mathbf{r}_{ij} \mathbf{r}^{\mathrm{T}}}{r_{ijij}}$$

Size and shape of the super-cell are changing

$g = h^{\mathrm{T}} h$, $\mathbf{v}_i = h \dot{\mathbf{s}}_i$ $\quad \sigma_{\alpha\beta} = \partial \Omega / \partial h_{\alpha\beta}$.

TB Method and molecular dynamics (TBMD)

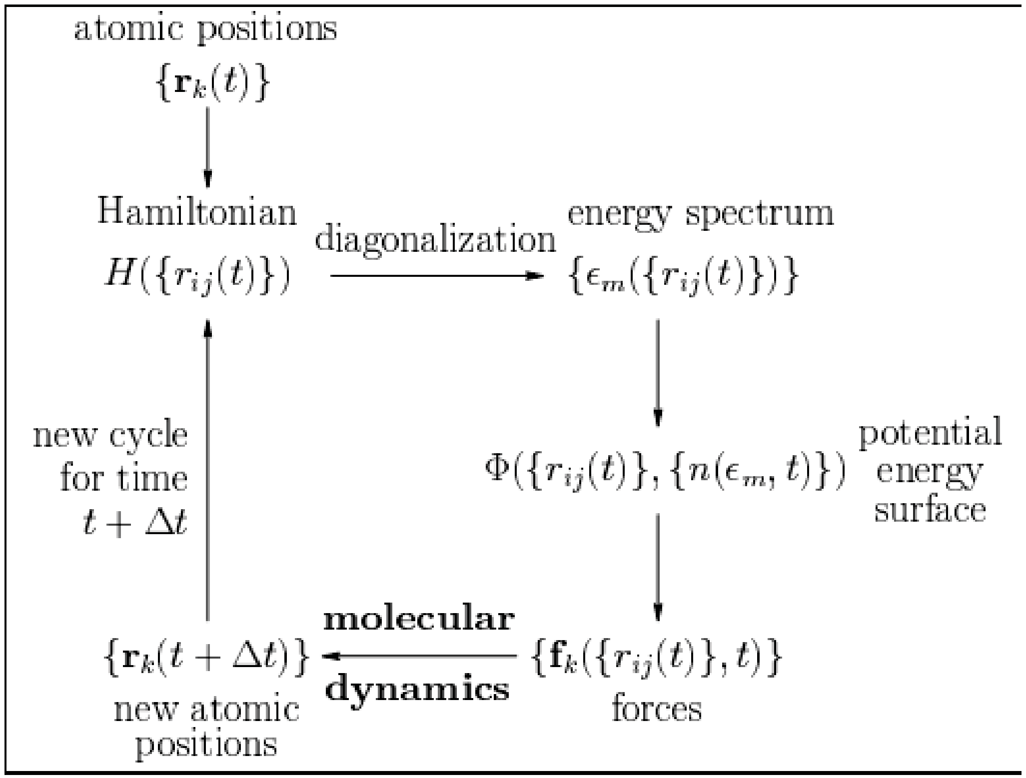

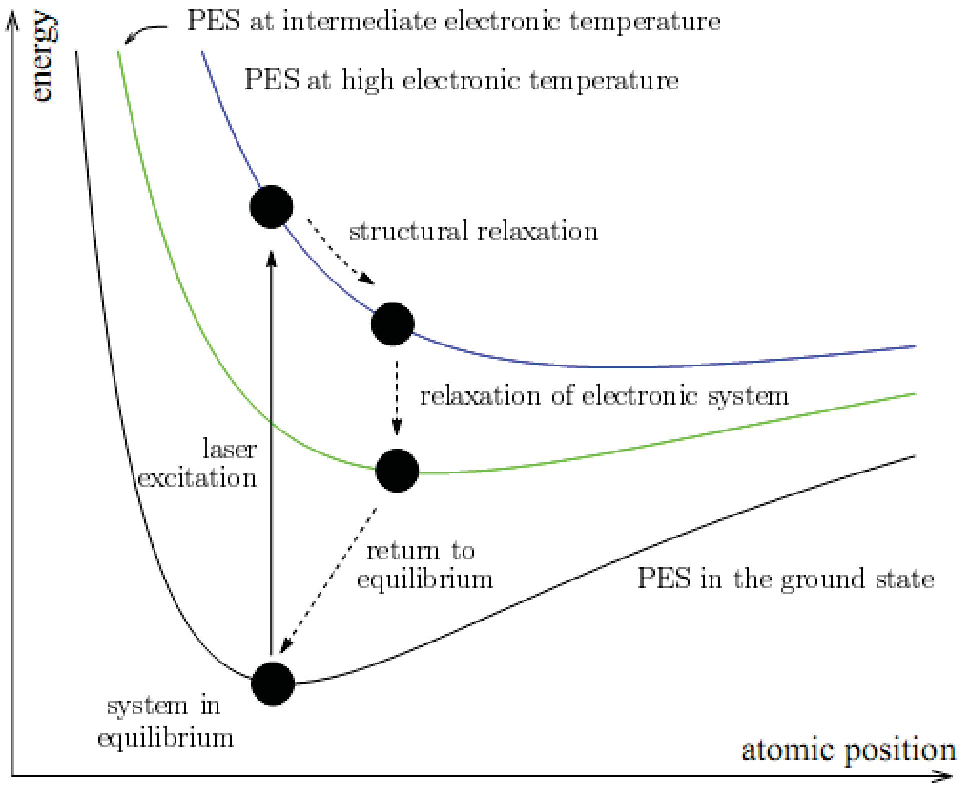

[H. Jeschke et al. PRL 1999]

TB Method and molecular dynamics (TBMD)

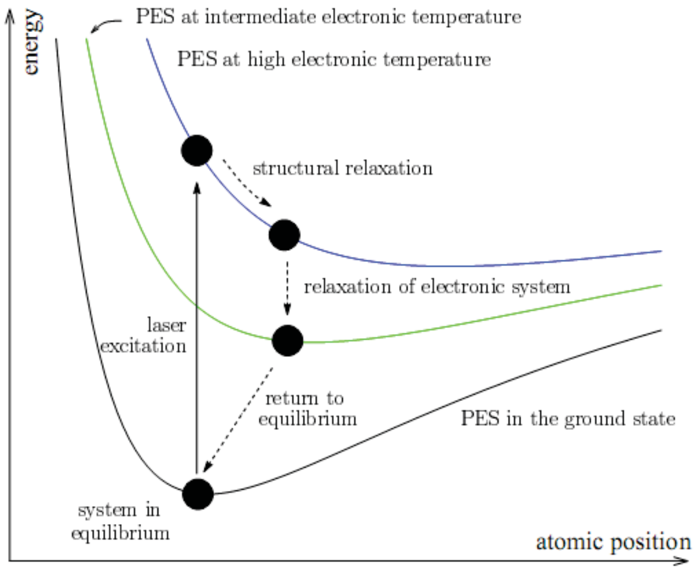

$$m_k \ddot{\mathbf{r}}_k = -\frac{\partial \Phi(\{r_{ij}\}, t)}{\partial \mathbf{r}_k}$$

Electrons **Core**

$$\Phi(\{r_{ij}(t)\}, t) = \underbrace{\sum_m f(\epsilon_m, t)\epsilon_m}_{\text{Electrons}} + \underbrace{\frac{1}{2}\sum_{\substack{ij\\ j\neq i}} E_{\text{rep}}(r_{ij})}_{\text{Core}}$$

***f*(ϵ_m,*t*) - transient electron distribution function**

$\epsilon_m(\{r_{ij}(t)\}) = \langle m|H_{\text{TB}}(\{r_{ij}(t)\})|m\rangle$ **- transient band structure**

[H. Jeschke et al. PRL 1999]

Combined MC-TBMD

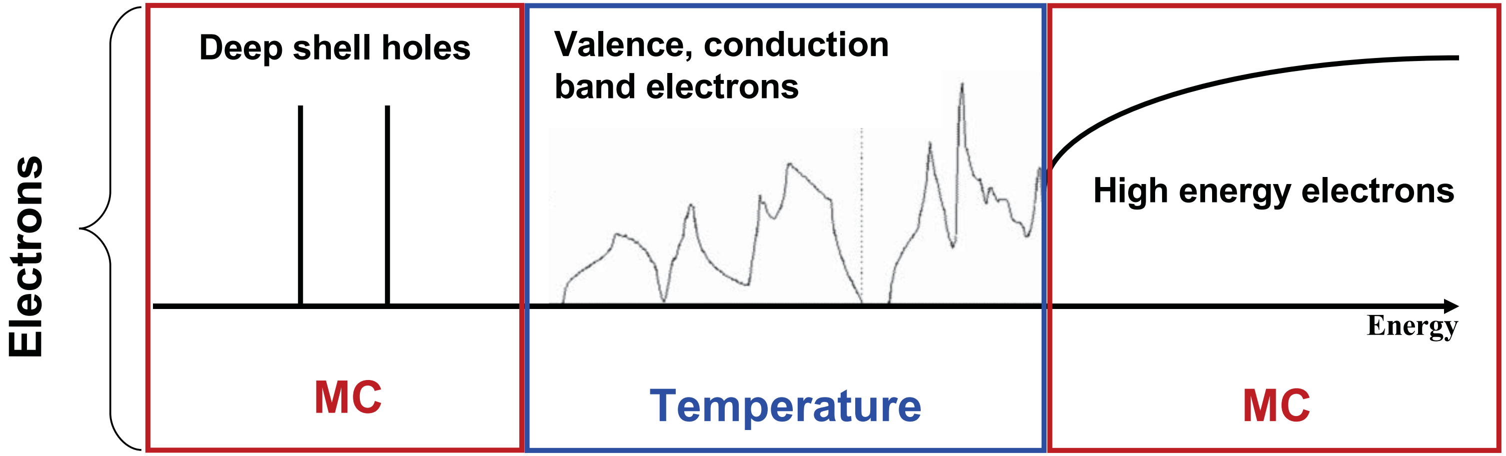

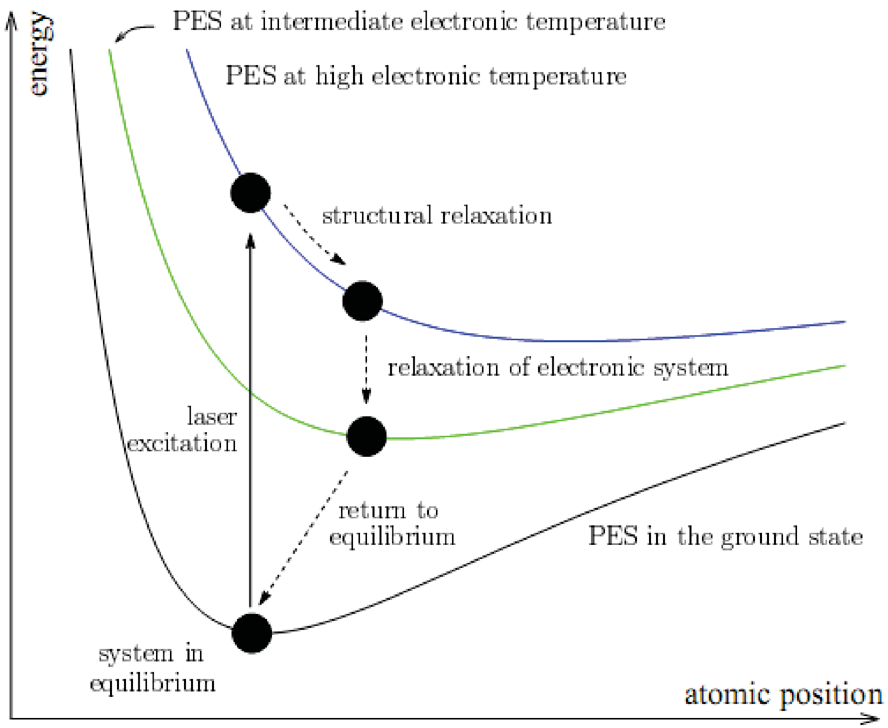

$$m_k \ddot{\mathbf{r}}_k = -\frac{\partial \Phi(\{r_{ij}\}, t)}{\partial \mathbf{r}_k}$$

Electrons Core

$$\Phi(\{r_{ij}(t)\}, t) = \underbrace{\sum_m f(\epsilon_m, t)\epsilon_m}_{\text{Electrons}} + \underbrace{\frac{1}{2}\sum_{\substack{ij \\ j \neq i}} E_{\text{rep}}(r_{ij})}_{\text{Core}}$$

[B. Ziaja, N. Medvedev, HEDP 8, 18 (2012)]

Processes considered

1) **Photoabsorbtion by deep shells and VB**

2) **Scattering of fast electrons:**

   - **Deep shells ionization**

   - **VB and CB scatterings**

1) **Auger-decays of deep holes**

} **- MC**

2) **Thermalization in VB and CB** — **- Temperature** (Boltzmann eq.)

3) **Lattice heating, atomic dynamics**

4) **Changes of band structure**

5) Changes of scattering rates (not included yet)

} **- TBMD**

Electron scattering cross-section

Scattering of strongly-correlated system:

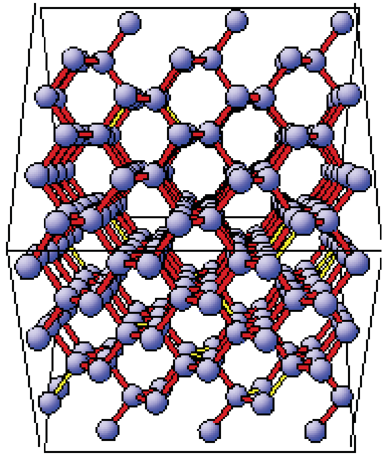

$$\frac{d^2\sigma}{d\Omega d\epsilon} = A\,\mathcal{S}(q,\omega),$$

$$A = \frac{m^2}{4\pi^2\hbar^5}\frac{k}{k_0}W(q),$$

$$\mathcal{S}(q,\omega) = \sum_{n_0} p_{n0} \sum_n \left| \left[\sum_{j=1}^{N} \exp(iq\cdot \mathbf{r}_j) \right]_{n0}^{n} \right|^2 \cdot \delta\left\{ \omega + \frac{E_{n0} - E_n}{\hbar} \right\},$$

[L. van Hove, Phys. Rev. 1954]

Electron scattering cross-section

$$\frac{d^2\sigma}{d\Omega d\epsilon} = A\,\mathcal{S}(q,\omega),$$

$$A = \frac{m^2}{4\pi^2\hbar^5}\frac{k}{k_0}W(q),$$

$$\mathcal{S}(q,\omega) = \sum_{n_0} p_{n_0} \sum_n \left| \left[\sum_{j=1}^{N} \exp(iq\cdot\mathbf{r}_j) \right]_{n_0}^{n} \right|^2 \cdot \delta\left\{ \omega + \frac{E_{n_0} - E_n}{\hbar} \right\},$$

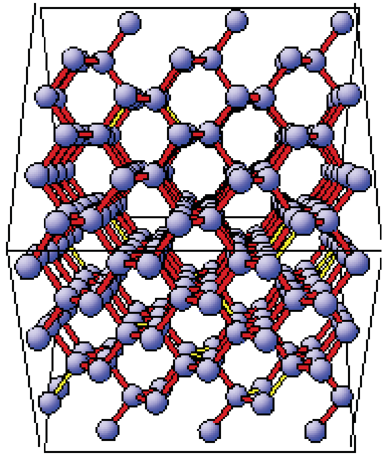

$$\mathcal{S}(q,\omega) = (2\pi)^{-1} N \int \exp[i(q\cdot\mathbf{r} - \omega t)]\cdot G(\mathbf{r},t)\,d\mathbf{r}\,dt,$$

Collective scattering, NOT individual binary encounters

[L. van Hove, Phys. Rev. 1954]

Electron scattering cross-section

$$\frac{d^2\sigma}{d\Omega d\epsilon} = A\,\mathcal{S}(q,\omega),$$

$$A = \frac{m^2}{4\pi^2\hbar^5}\frac{k}{k_0}W(q),$$

$$\mathcal{S}(q,\omega) = \sum_{n0} p_{n0} \sum_{n} \left| \left[\sum_{j=1}^{N} \exp(iq\cdot\mathbf{r}_j) \right]_{n0}^{n} \right|^2 \cdot \delta\left\{ \omega + \frac{E_{n0} - E_n}{\hbar} \right\},$$

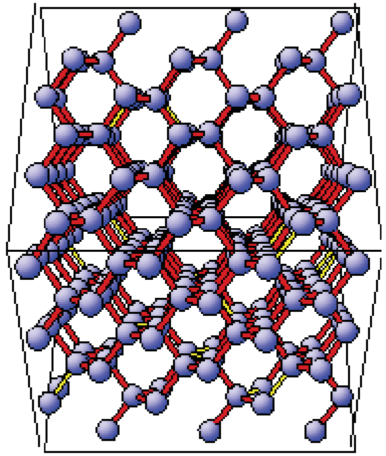

Fluctuation-dissipation theorem:

$$S(\mathbf{q},\omega) = \frac{q^2}{4\pi^2 n}\,\mathrm{Im}\left(\frac{1}{\varepsilon(\boldsymbol{q},\omega)}\right)$$

$$\frac{\mathrm{d}\lambda^{-1}}{\mathrm{d}(\hbar\omega)} = \frac{2Z_{\mathrm{eff}}^2 e^2}{\pi\hbar^2 v^2}\int_{q_-}^{q_+} \mathrm{Im}\left[\frac{-1}{\varepsilon(\boldsymbol{q},\omega)}\right]\frac{\mathrm{d}q}{q}$$

[R. Kubo, Rep. Prog. Phys. 29, 255 (1966)]

Complex dielectric function (CDF)

Plasmon spectra: $\varepsilon(\boldsymbol{q},\omega) = 0$

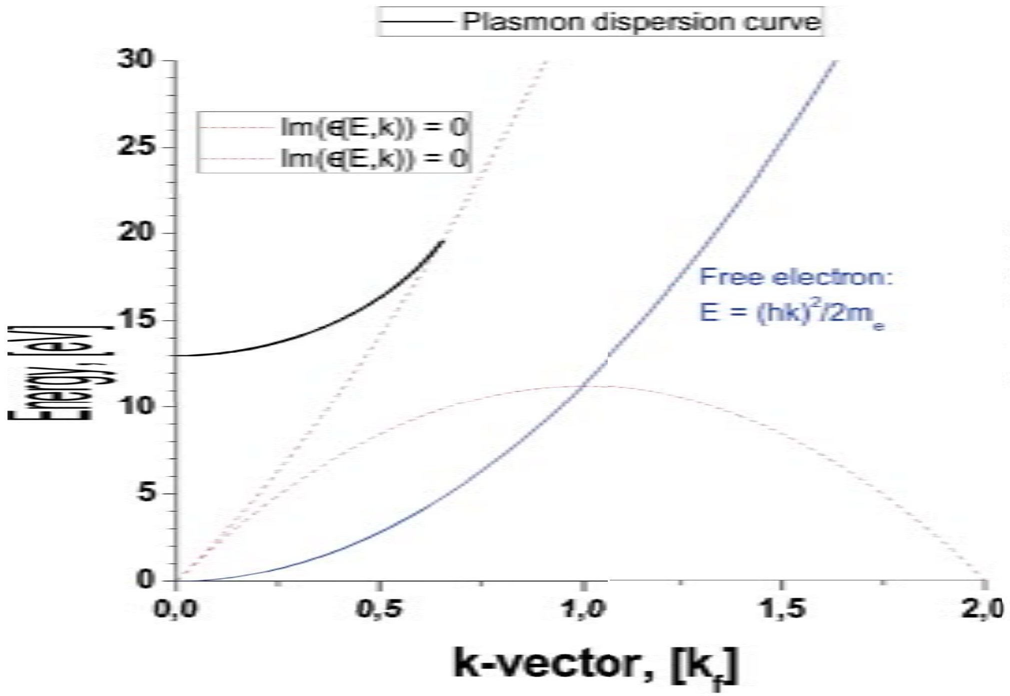

CDF accounts for collective behavior of electrons

Screening effects

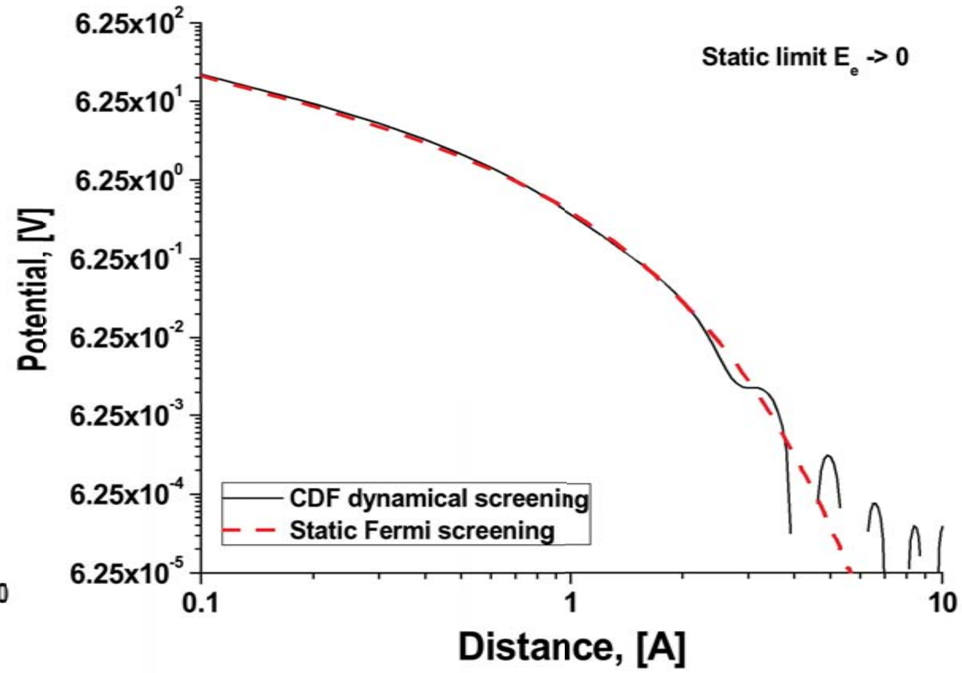

CDF gives dynamical screening

[N.W. Ashcroft, N.D. Mermin, "Solid State Physics"]

Cross-section and complex dielectric function

$$\frac{d\lambda^{-1}}{d(\hbar\omega)} = \frac{2Z_{\text{eff}}^2 e^2}{\pi\hbar^2 v^2} \int_{q_-}^{q_+} \text{Im}\left[\frac{-1}{\varepsilon(\boldsymbol{q},\omega)}\right] \frac{dq}{q}$$

Dielectric function calculated out of TBMD:

$$\epsilon(\omega) = \left[1 - \frac{\omega_p^2}{\omega^2}\right] - \frac{4\pi e^2}{\Omega m_e^2 \omega^2} \sum_{ij} \frac{(n_i - n_j)}{\epsilon_i - \epsilon_j - \hbar\omega} \left|\langle i|\hat{p}_E|j\rangle\right|^2$$

Transient electron distribution

Transient energy levels

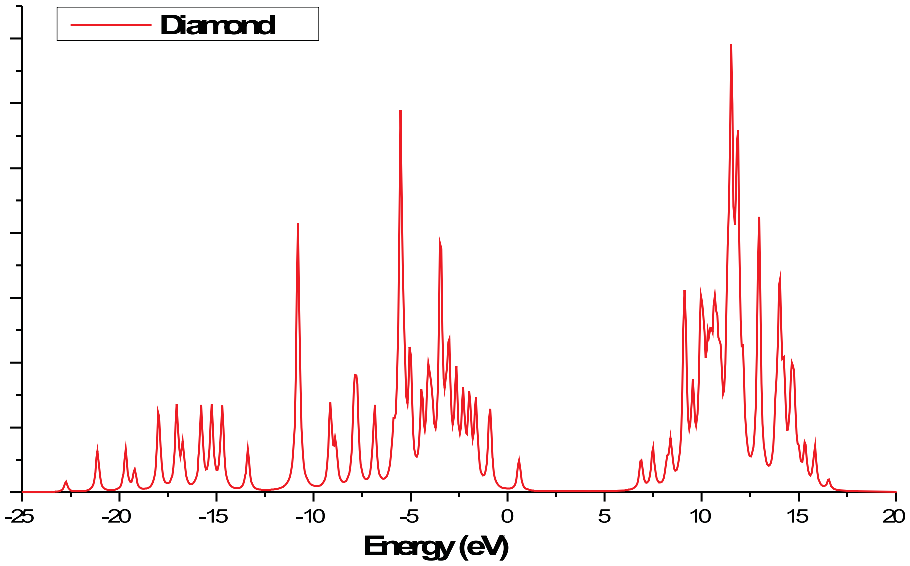

Example: nonthermal melting of semiconductors

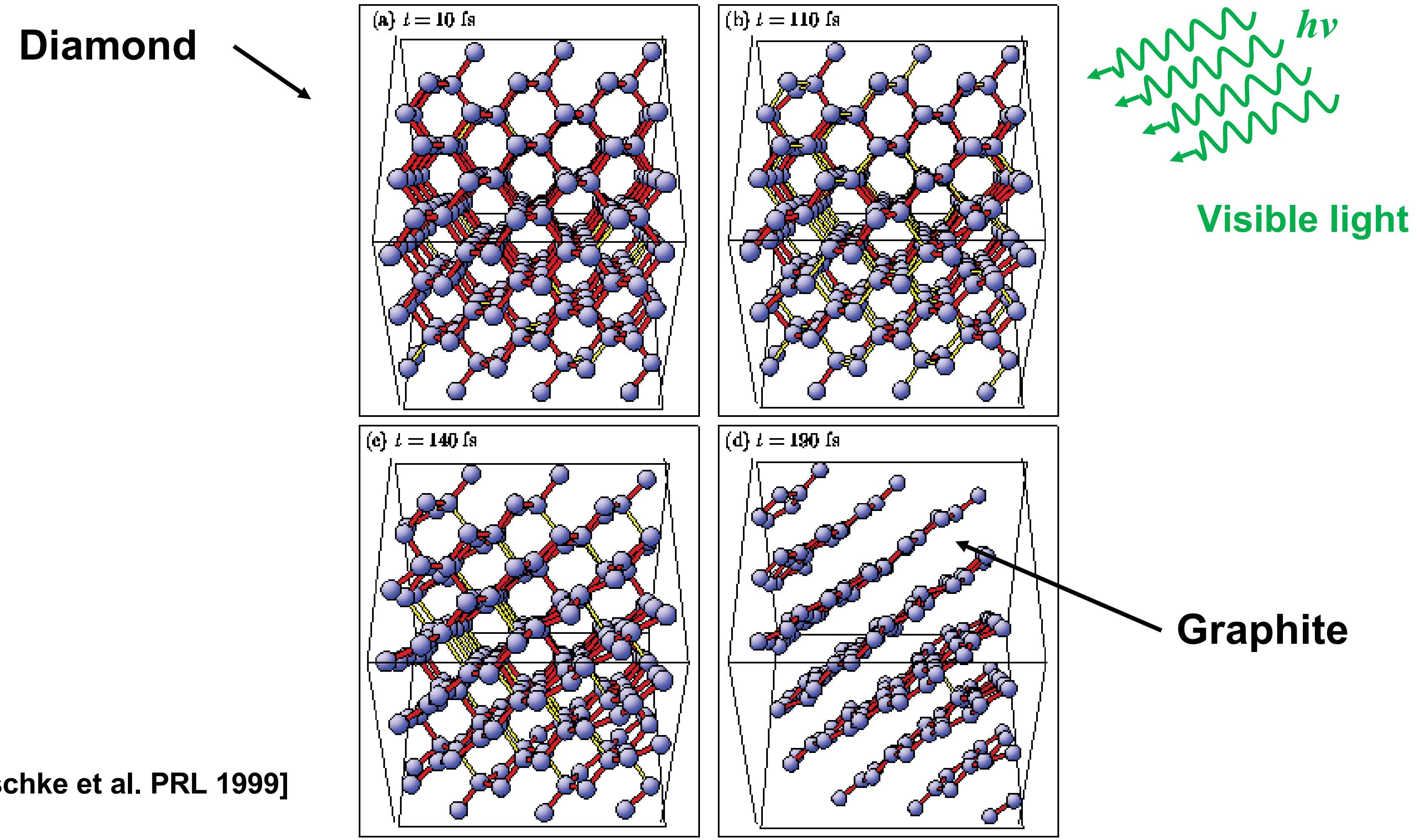

[H. Jeschke et al. PRL 1999]

Ultrafast phase transition due to a change of interatomic potential

Preliminary results from the model

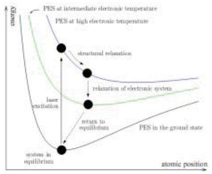

1) **New hybrid model is developed: MC-TBMD**

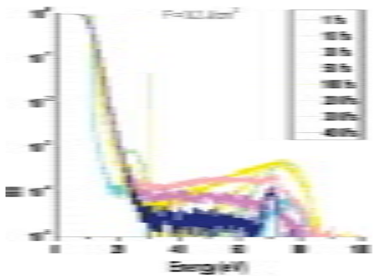

2) **Typical electron distribution "bump on hot tail":**
   - **Thermalized low energy part**
   - **Non-thermalized high energy tail**

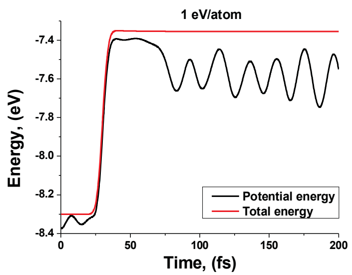

3) **Transition from diamond to graphite afte FLASH irradiation within 100 fs**

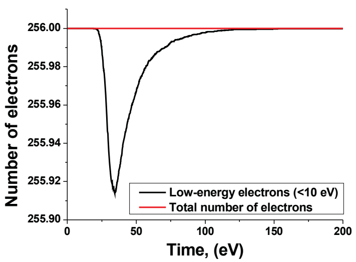

4) **Nonthermal melting, not a Coulomb explosion**

III. Summary and Outlook

Summary

- Various mechanisms of radiation induced dynamics
- Models: particle approach → spatiotemporal characteristics of Auger-electron cascades in solids with MC code
- Models: transport approach → Boltzmann code: so far the only model that gives an accurate description of all of the experimental data from atomic clusters at 100 nm and 32 nm wavelength. Also in good agreement with data from warm dense matter hydrogen experiment at 13 nm → describes data as experiments are progressing

Conclusions

- Understanding of radiation damage within FEL irradiated solids important for theory and experiment

- Choice of the method for modelling the radiation damage depends on the structure of the sample, photon energy and pulse fluence

- Modelling of structral changes requires combined approach with particle methods: MC, MD, transport methods:Boltzmann equation, following the evolution of band structure:TB/DFT

Atomic Data: Necessary Input!

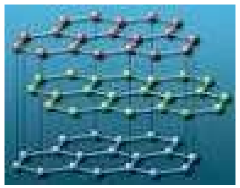

CFEL SCIENCE

DESY

Perspectives for:
Following Non-equilibrium Dynamics

Further developments for Boltzmann code:

- **Various structures** (heterogeneous, magnetic, solids→ following the evolution of band structure)
- Going beyond **the limitation of spherically symmetric samples**
- Upgrade to **X-ray wavelength**
- Going beyond **classical treatment** → description of dense/degenerate systems
- Fast hybrid code **for coherent diffraction imaging simulations**
- Going beyond **single particle density** → correlated systems

Investigations of
Laser-created Plasmas

Following the non-equilibrium evolution of laser-created plasmas

- **Transport properties**
- **Effects of charged plasma environment**
- **Exotic states (e.g. light-transparent plasmas)**
- **High intensity limit**
- **Equation of state in WDM**

THANKING MY COLLABORATORS ...

C. Bostedt (SLAC)

H. Chapman (CFEL)

H. Jeschke (U. Frankfurt)

N. Medvedev (CFEL)

T. Möller (TU Berlin)

R. Santra (CFEL)

F. Wang (CFEL)

E. Weckert (HASYLAB)

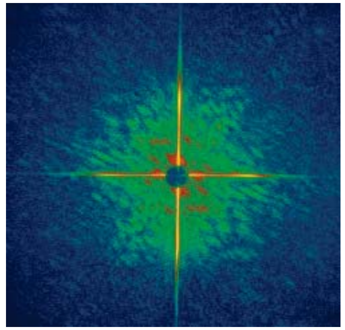

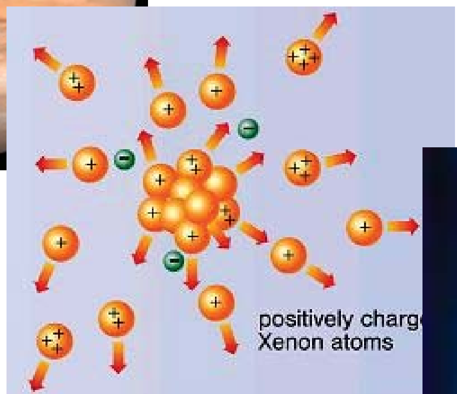

HELMHOLTZ
ASSOCIATION

CFEL SCIENCE

DESY

The cluster experiment group

Technische Universität Berlin

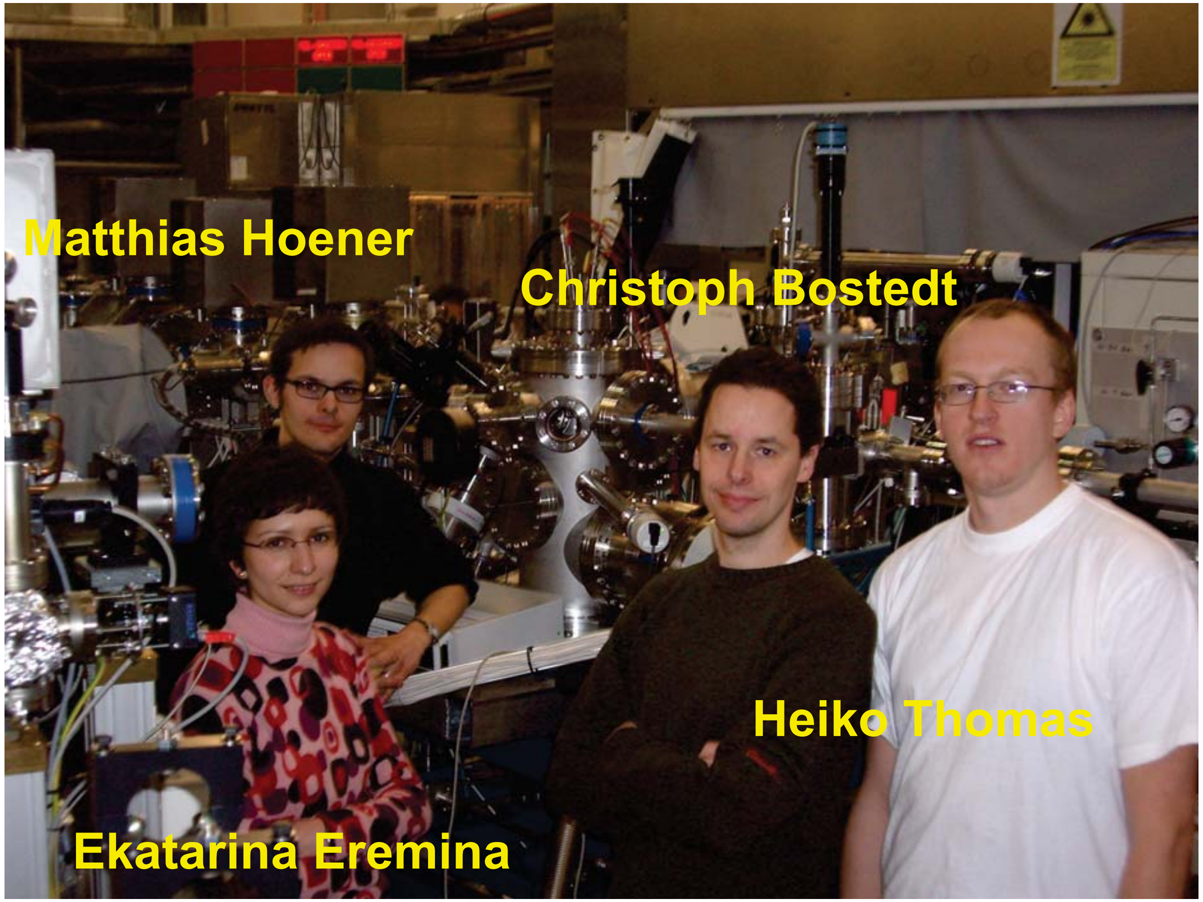

Thomas Möller

Funding:
BMBF, HGF

Special thanks to
R. Treusch, S. Düsterer, J. Feldhaus
and the FLASH control room Team

Collaboration
with the groups of J. Hajdu (Uppsala, Stanford)
and H. Chapman (CFEL)
R. Hartmann, C. Reich, L. Strüder, MPG Halbleiterlabor

Peak Brightness Collaboration

- **DESY, Hamburg**
  S. Düsterer, R.R. Fäustlin, T. Laarmann, H. Redlin,
  N. Stojanovic, F. Tavella, S. Toleikis, T. Tschentscher
- **University of California, Berkeley**
  H.J. Lee
- **University of Jena**
  E. Förster, I. Uschmann, U. Zastrau
- **LLNL, Livermore**
  T. Döppner, S.H. Glenzer
- **University of Oxford / RAL, Chilton, Didcot**
  G. Gregori, B. Li, J. Mithen, J. Wark
- **University of Rostock**
  T. Bornath, C. Fortmann, S. Göde, R. Irsig,
  K.-H. Meiwes-Broer, A. Przystawik, R. Redmer,
  H. Reinholz, G. Röpke, R. Thiele, J. Tiggesbäumker

Helmholz Association: VH-VI-104; **Science and Technology Facilities Council UK**;
German Research Foundation: GRK 1355, SFB 652, LA 1431/2-1; **DOE**: DE-AC52-07NA27344,
LDRDs 08-ERI-002, 08-LW-004; **German Ministry for Education and Research**: FSP 301-FLASH;
European Community: RII3-CT-2004-506008 (IA-SFS)

FLASH FEL at DESY

User Facility started 2005

Now after upgrade 2009...

- 4,5- 50 nm
- 10-100 μJ
- 5 GW_{peak}
- 10-100 fs

Plasma created by VUV photons

Example:

Xenon clusters → atomic density, $n_A = 10^{22} - 10^{23}$ cm^{-3} → estimated electron density $n_e = 10^{22} - 10^{24}$ cm^{-3} → dense plasma

Photoelectron energies, $E_{ph}(\lambda = 98\ nm) \approx 0.6$ eV
$E_{ph}(\lambda = 32\ nm) \approx 26.6$ eV

↓

Temperature of emitted photoelectrons,
$T_{ph}(\lambda = 98\ nm) \approx 0.4$ eV ← cold plasma
$T_{ph}(\lambda = 32\ nm) \approx 17.6$ eV ← warm plasma

Inverse bremsstrahlung

Average energy gain per unit time

$$\left\langle \frac{d\mathcal{E}_0}{dt} \right\rangle_i = \frac{n_i i^2 e^4}{4\pi\epsilon_0^2} \left\langle \frac{\mathbf{uv}}{v^3}\, ln\,\Lambda \right\rangle$$

where:

n_i, ion density in plasma

$ln\,\Lambda$, Coulomb logarithm dependent on cut-offs, $ln\,\Lambda \sim ln\,(b_{max}/b_{min})$, $b_{max} = v/\omega$, $b_{min} = max(\lambda_{Broglie}, b_{90^\circ})$

i, charge of a point-like ion